

https://dspace.org/

Investigation of the Ramotswa Transboundary Aquifer area, groundwater flow and pollution

Modisha, Reshoketswe Caroline Oudi

2017

http://hdl.handle.net/10539/23568

Modisha, Reshoketswe Caroline Oudi (2017) Investigation of the Ramotswa Transboundary Aquifer Area, groundwater flow and pollution, University of the Witwatersrand, Johannesburg, <http://hdl.handle.net/10539/23568>

Downloaded from a DSpace repository. https://dspace.org/

Investigation of the Ramotswa Transboundary Aquifer Area, groundwater flow and pollution

Reshoketswe Caroline Oudi Modisha

Student number - 305275

GEOL 7028 - Research report

In partial fulfillment for Master of Science in Hydrogeology

School of Geosciences

University of the Witwatersrand



WITS
UNIVERSITY

June 2017

PLAGIARISM DECLARATION POLICY

Declaration by Student

I **Reshoketswe Caroline Oudi Modisha** Student number: **305275** am a student registered for **M.Sc. in Hydrogeology** (course work and research report) in the year **2016**. I hereby declare the following:

I am aware that plagiarism (the use of someone else's work without their permission and/or without acknowledging the original source) is wrong.

I confirm that ALL the work submitted for assessment for the above course is my own unaided work except where I have explicitly indicated otherwise.

I have followed the required conventions in referencing the thoughts and ideas of others.

I understand that the University of the Witwatersrand may take disciplinary action against me if there is a belief that this is not my own unaided work or that I have failed to acknowledge the source of the ideas or words in my writing.

Signature: R.C.O. Modisha Date: **2 June 2017**

Acknowledgements

This study would not have been possible without the financial support from Golder Associates Empowerment Trust Bursary Scheme. My sincere gratitude goes to Prof. Abiye, my supervisor and lecturer, for allowing me to be part of the Masters in Hydrogeology program and in turn allowing me to pursue my dream and to be of service to my community. I would also like to thank him for his enthusiasm for the science which has easily turned into my passion. I am especially indebted to Yvan Altchenko and Karen Villholth for giving me the opportunity to work on one of the many projects at International Water Management Institute Southern Africa office together with their generous staff, Girma Ebrahim and Manuel Magombeyi, and for providing resources to see this project through. This study was conducted as part of GRECHILM project (PEER) financed by the National Academy of Sciences (USA) and Department of Science and Technology (RSA). My family has been truly supportive of me in my pursuit of my studies. I would like to thank my parents and Karabo Kgomongwe for the emotional support, guidance and words of encouragement along the way.

ABSTRACT

Groundwater is a principal source of water for many semi-arid countries, including Botswana and South Africa. This is especially true for the rural communities within these regions that lie on the periphery of local water scheme pipelines and make direct use of groundwater. The Ramotswa transboundary aquifer, which supplies local communities and nearby cities with fresh groundwater, is a highly productive and unique karst sequence shared by South Africa and Botswana. The objective of the study was to contribute to the available hydrogeological data by means of evaluating groundwater flow, nitrate pollution and the median recession index and master recession curve for the aquifer. The interpreted airborne geophysical data revealed the presence of collapsed features in the northeastern area corresponding to the karst morphology. A piezometric map of the area shows the groundwater flow is towards the north-northeast, which is supported by salinity increase across the study area. Increased nitrate concentrations were identified in areas with increased rainfall, shallow groundwater and a mature karst system. Only 3% of the 36 sample sites had nitrate concentrations exceeding the WHO guideline limit of 50 mg/l. This was attributed to the legacy of unlined pit latrines in karstified areas. Pollution is entirely anthropogenic and generally from non-point sources. A median recession index computed by RECESS program from the Dinokana spring discharge data was 295.7 days per log cycle and the generated master recession curve's gentle slope alludes to massive storage potential within the karst compartment. The results of the study can alert stakeholders alike of the health risk of direct consumption of the groundwater without pretreatment. Establishing an understanding of the nitrate pollution sources and groundwater flow direction, and estimating the recession index provides informed groundwater pollution and vulnerability management options. This can improve the aquifer resource assessment and the livelihoods of local communities in the face of increasing climate change.

TABLE OF CONTENTS

Acknowledgements iii

ABSTRACT iv

LIST OF FIGURES vii

LIST OF TABLES viii

1 INTRODUCTION 1

1.1 Aims and Objectives 2

1.2 Aim 2

1.3 Objectives 3

2 LITERATURE REVIEW 4

2.1 Geology 4

2.2 Regional tectonic influence in study area 5

2.3 Structural geology 6

2.4 The Transvaal Supergroup and lithostratigraphy 8

2.4.1 Black Reef Formation 9

2.4.2 Chuniespoort Group 9

2.5 Hydrogeological setting 13

2.5.1 Water levels and flow direction 15

2.6 Karst development 15

2.6.1 Geomorphology 16

2.6.2 Karst aquifer characteristics 17

2.6.3 Compartmentalization of the Transvaal karst aquifer 18

2.7 Groundwater Pollution 19

2.7.1 Environmental fate of nitrate 20

2.7.2 Drinking water quality standards 22

3 STUDY AREA 23

3.1.1 Water supply and sanitation 24

3.1.2 Physiography 24

3.1.1 Climate 25

3.1.2 Sub-catchments of the Limpopo River Basin system 27
3.1.3 Dinokana Spring 28
4 METHODOLOGY 30
4.1 Data sources 30
4.2 Sampling sites 30
4.3 Water level measurement 31
4.4 Piezometric map construction 32
4.5 Groundwater sampling 32
4.6 Analytical Methods 33
4.7 Microbiological investigation 34
4.8 Quality assurance and Control 35
4.9 Physio-chemical analysis 35
4.10 Identification of potential groundwater pollutants 35
4.11 Nitrate pollution map 36
4.12 Airborne Electromagnetic (AEM) data acquisition and interpretation 36
4.13 Spring hydrograph analysis using RECESS program 37
4.13.1 Description of the method 38
4.13.2 Determination of Recession Index (K) and Master Recession Curve (MRC) 39
5 RESULTS AND DISCUSSION 40
5.1 Quality assurance and control 40
5.2 Piezometric map 40
5.3 Groundwater pollution 44
5.4 Nitrate pollution sources 46
5.5 Groundwater pH 51
5.6 Interpreted airborne geophysical survey results 53
5.7 Recession index (K) estimate 56
5.8 Master recession curve 56
6 CONCLUSION 58
7 RECOMMENDATIONS 59
8 REFERENCES 60

Appendix A: Well site description 66

Appendix B: Water level sites and readings 69

Appendix C: Nitrate + Nitrite, E Coli, Total Coliform values of sample sites 70

Appendix D: In situ field parameters 71

Appendix E: CURV output 72

LIST OF FIGURES

Figure 1. Distribution of the Chuniespoort group within the structural basins, modified from Moore *et al.* (2001). 5

Figure 2. The orientation of faults within the study area (source: Council for Geoscience; Botswana Geoscience Institute) 7

Figure 3. Folded shale outcrop along the N4 route toward the Skilpadhek border, South Africa. 8

Figure 4. Dolomite with interbedded chert dipping at 36˚ south east found in the south-western region of the study area, South Africa. 10

Figure 5. Simplified geological map of the study area (source: XRI Blue, 2016) 12

Figure 6. Diagram of a karst conceptual model illustrating duality of: recharge, infiltration and flow (Goldscheider *et al.*, 2007). 18

Figure 7. The fate of nitrate in the environment (Source: Staudt, 2003). 21

Figure 8. Location of the Ramotswa Transboundary Aquifer Area. 23

Figure 9. Digital elevation map for the study area, indicating the highest and lowest elevation at about 1 334 mamsl and 1 025 mamsl respectively. 25

Figure 10. Position of the rainfall stations in and around study area (Altchenko *et al*., 2016). 26

Figure 11. Comparison of monthly rainfall across rainfall stations (Source: Altchenko *et al.,* 2016). 27

Figure 12. Notwane catchment within the Limpopo River Basin 28

Figure 13. Dinokana upper eye flow record 1990 - 2015 (Altchenko *et al.,* 2016). 29

Figure 14. Sample location for water quality analysis. 31

Figure 15. Well purging after uncapping the borehole. 33

Figure 16. Illustration of an airborne electromagnetic survey (source: XRI Blue, 2016). 37

Figure 17. Methods used to determine the master recession curve (MRC): (A) Selected recession segments, (B) Recession index (K) and best fit line (C) Master Recession Curve derived from coefficients in B (Rutledge, 2007). 39
Figure 18. Correlation graph between water level and elevation. 41
Figure 19. Piezometric map of the study area and indication the groundwater flow direction. 42
Figure 20. Spatial distribution of the total dissolved solids in the study area..... 43
Figure 21. Spatial distribution of the sum of nitrate and nitrite..... 45
Figure 22. Comparison of the nitrate concentration values in boreholes in the years 2011, 2012 (DWA) and 2016. 46
Figure 23. Sample site ODI03ZA showing the position of the community water tank near an abandoned animal kraal. 47
Figure 24. *E. Coli* counts at sample sites by (A) CFU/100 ml and (B) MPN/100 ml 49
Figure 25. Total coliform count at sample sites by (A) CFU/100 ml and (B) MPN/100 ml. 50
Figure 26. Goat kraal situated directly where private borehole is drilled in a highly karstified area (Supingstad, South Africa)..... 51
Figure 27. The water reaction (pH) levels at sample sites. 52
Figure 28. Remnant magnetic field of the fly zone in the study area (Source: XRI Blue, 2016). 54
Figure 29. Interpreted collapsed features in the study (source: Council for Geoscience; Botswana Geoscience Institute; XRI Blue). 55
Figure 30. Master Recession Curve for the Dinokana spring from recession segments between 1990-2015; The regression slope reflects the storage characteristics. 57

LIST OF TABLES

Table 1. Simplified lithostratigraphic column of the study area modified from (Eriksson *et al.,* 1993; Eriksson *et al*., 1995; Meyer, 2014). 11
Table 2. Correlation of the Transvaal and Bushveld Basin in the South East District in Botswana and South Africa (modified from Eriksson *et al.,* 1993). 13
Table 3. Summary of the Aquifer's hydrogeological properties (Staudt, 2003). 14
Table 4. A comparison of nitrate guideline value for drinking water with country standards. 22
Table 5. Summary of the in-situ field Parameters..... 52

1 INTRODUCTION

Groundwater plays a crucial role in supplying water to people across the world with 25% of this population drinking water from karst groundwater resources (Ford and Williams, 1989). In semi-arid countries groundwater is a principal and an invaluable water resource. This is because of insufficient surface water availability due to unpredictable rainfall and excessive evapotranspiration rates. South Africa and Botswana are semi-arid countries where groundwater resources provide relatively drought proof water supply for agriculture, mining, tourism and domestic use (Villholth *et al.,* 2013). Increasing population growth and climate variability experienced by both countries has led to significant use of groundwater and hence putting greater stress than ever before on the groundwater resources.

South Africa and Botswana share a highly productive karst aquifer called the Ramotswa dolomitic aquifer. This aquifer is located in the North West Province of South Africa and in the South East district in Botswana. This transboundary aquifer could be the solution to the water problems faced by the communities living in and around the transboundary area. Understanding and assessment of the groundwater systems in this transboundary aquifer area could provide a basis for improved decisions regarding the management of this precious groundwater resource for the benefit of both member states.

Nitrate has been identified by several authors as a widespread pollutant in groundwater around the world and has perilous health implications for both infants and adults when exposed to high concentrations (Kaçaroğlu and Günay, 1997; WHO,1998; Stadler *et al.,* 2012). In order to protect our groundwater resources, we need to be able to distinguish the sources of nitrate to give stakeholders a degree of the vulnerability of the groundwater supply. This is the first step to facilitate a possible management plan that could save countless lives, particularly in rural areas that rely directly on the groundwater resource (Gieske and Goud, 1994). Nitrate pollution is a wide spread problem in the village of Ramotswa in Botswana (Ranganani *et al*., 2001) and in South Africa very limited data exist on the pollution sources within the Ramotswa transboundary aquifer area.

The recent drought of 2015 affected both South Africa and Botswana. According to Steyn (2015) this was an El Niño induced drought that had caused the drying up of Gaborone dam and resulted in a cut in water supply from a South African dam in the North West Province to Botswana. Monitoring of groundwater levels provides useful data about changes

in the resource over time to forecast trends, such as groundwater flow direction, that can be beneficial for groundwater management efforts.

The importance of this study is to support the *Resilience in the Limpopo Basin: The potential role of the transboundary Ramotswa Aquifer* project by coordinating scientific knowledge in hydrogeology and groundwater pollution with the aim of improving livelihoods and highlighting the importance and vulnerability of the Ramotswa Transboundary Aquifer. The purpose of this study is to bridge the gap in current data, compare and harmonize data collected across the borders of South Africa and Botswana in order to construct a potentiometric map for the study area, understand the characteristics of the aquifer and determine the source attribution of nitrate in the transboundary aquifer area so that appropriate groundwater management strategies can be developed and applied.

1.1 Aims and Objectives

In terms of the information analysis undertaken by Altchenko *et al.* (2016), several information gaps were identified in the study of the Ramotswa Transboundary Aquifer. These information gaps prompted investigation into: (1) Aquifer characteristics by analysis of spring recession. This is a convenient and cost effective method that doesn't require detailed groundwater and watershed knowledge and was based solely on daily spring discharge records. The Dinokana spring, which forms a part of the Malmani Subgroup dolomitic sequences (i.e. the Ramotswa aquifer) was investigated. (2) Water level data; available data, particularly on the South African side of the study area, obtained from the Department of Water and Sanitation South Africa lacked water level readings for the boreholes across the study area recorded in the same year, making it unfeasible to construct a piezometric map of the study area before this study was carried out.

1.2 Aim

The aim of this study is to improve the understanding of the aquifer and contribute hydrogeological data to the Ramotswa transboundary aquifer area in order to promote better groundwater governance in one of the most significant shared aquifers in the Limpopo River Basin.

1.3 Objectives

In order to achieve the study's aim, the study is guided by the following specific objectives:

- To produce a piezometric map in order to understand and determine the overall ground water flow direction across the Ramotswa Transboundary Aquifer.
- To map the nitrate pollution in the transboundary area and deduce its source.
- To estimate the recession index of the aquifer based on historical spring discharge data using RECESS program and analyze the airborne geophysical survey interpretation results.
- To give recommendations for improved groundwater monitoring and protection in study area.

2 LITERATURE REVIEW

2.1 Geology

The late Archean to early Proterozoic Transvaal Supergroup is well-preserved within three structural basins on the Kaapvaal Craton (Eriksson *et al.,* 2006). The Transvaal/Bushveld in South Africa and Kanye Basin in Botswana are where the study is situated. Eriksson *et al.* (1993) and Eriksson *et al.* (2006) notes the striking similarity in the successions found in these structural basins with the best correlation identified for the lower chemical sedimentary units. This study focuses on the Chuniespoort Group of the Transvaal Supergroup, which hosts this study's target geological unit, the Malmani Subgroup, also known as the Ramotswa dolomitic aquifer.

The study area overlies the north-western part of the Kaapvaal Craton. The mapped surface geology, Chuniespoort chemical sedimentary unit, forms an arcuate on the western flank of the Transvaal basin (Figure 1). According to Walraven (1990) the Chuniespoort and Pretoria Groups were intruded by the Bushveld Complex around 2.06 Ga (Giga-annum) with several mafic sills and dykes. The carbonates in the Transvaal basin have been affected to a limited extent by the metamorphism as a result of the intrusion of the Bushveld Complex (Button, 1986). The Bushveld Complex intrusion produced classical contact metamorphic lithologies by forming hornfels in fine siliciclastic rocks (Martini *et al.*, 1995). With the Bushveld being a hypabyssal intrusion, the metamorphic grade decreased stratigraphically in descending order away from the intrusion and in places this metamorphism extended deep enough to affect the upper part of the Malmani Subgroup (Martini *et al.*,1995).

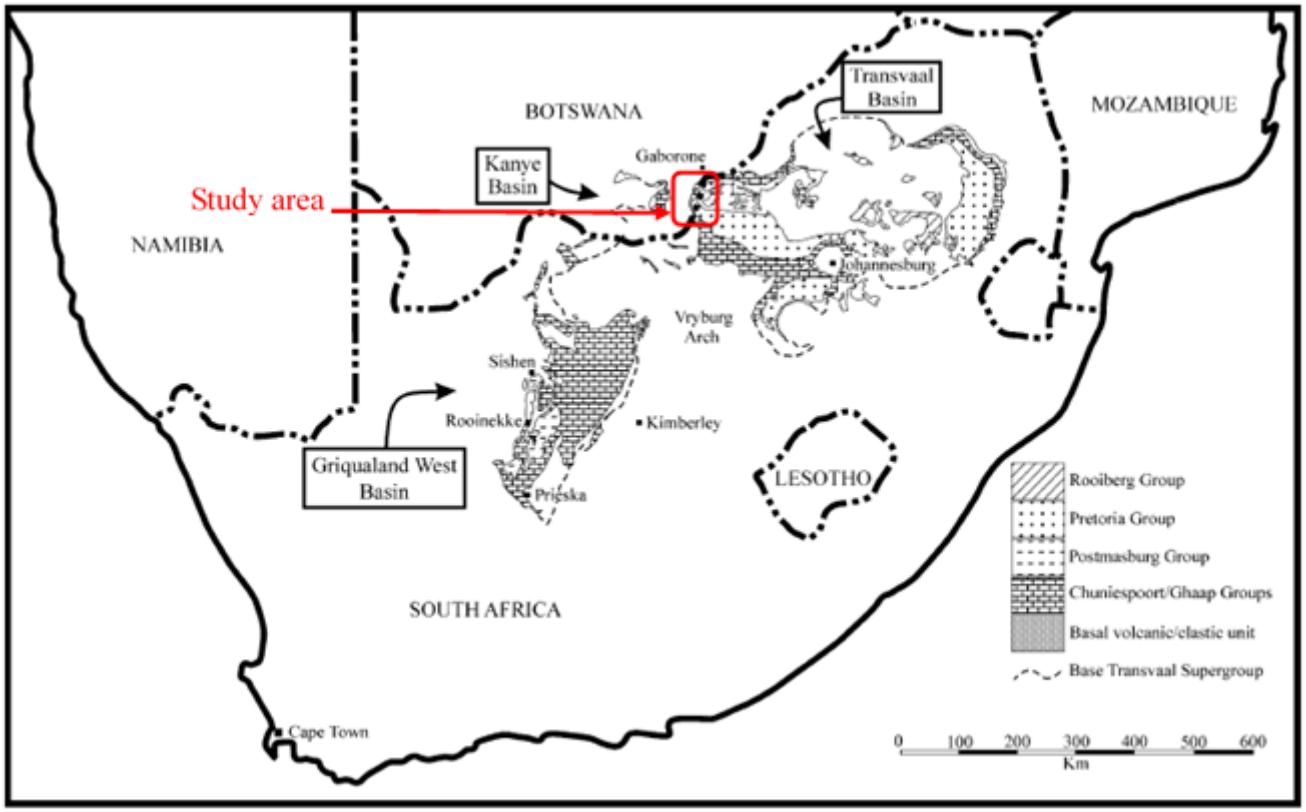

Figure 1. Distribution of the Chuniespoort group within the structural basins, modified from Moore *et al.* (2001).

2.2 Regional tectonic influence in study area

The suturing of the Kaapvaal and the Zimbabwe Cratons generated periods of regional compression (Clendenin *et al*., 1988). According to Burke *et al.* (1985) this collision seems to be between an Atlantic-type margin development on the southern boundary of the Zimbabwe Craton and on an Andean-type boundary on the Kaapvaal Craton. Dewey and Burke (1973) identified this suture between the Zimbabwe and Kaapvaal Cratons with characteristic east-northeast trending line of sheared rocks such as amphibolitic and peridotitic gneisses related to riebeckite gneisses and granulites. According to Clendenin *et al.* (1988) the oblique collision generated regional tensional stresses that drove the Kaapvaal three-stage divergent rift system. The Ventersdorp Supergroup sedimentary and volcanic rocks were then later deposited in these north to northeast trending grabens that are associated with the earlier collision of the two Cratons (Burke *et al.*, 1985).

According to Clendenin (1989) simple tectonic style (neither extensional nor compressional stress dominates) is identified as a mechanism that influenced numerous Early

Proterozoic successor basins on the Kaapvaal Craton and is interpreted from stress fields from Ventersdorp Supergroup through Transvaal sea time. Clendenin *et al.* (1988) and Clendenin (1989) have attributed the saucer shaped Kaapvaal basin in which the Chuniespoort Group accumulates to be a result of thermal subsidence.

2.3 Structural geology

Contrary to the structural analysis made by Key (1983), Dietvorst (1988) revealed new data on the structural setting of the study area in south eastern Botswana. This new data on the tectogenesis interpreted by Dietvorst (1988) suggests that the rocks of the Transvaal Supergroup were deposited in one sedimentary basin that extended into Botswana. Faulting followed by regional folding in an easterly to east-northeasterly plunging axes (F_1) is evident in the villages of Ramotswa and Lobatse and refolding about south-southeasterly axes (F) resulted in basement updoming and block faulting of the underlying supracrustal rocks (Dietvorst, 1988). Tectonic activity had ended before Waterberg sediments were deposited (Dietvorst, 1988). These structural events that took place in the study area are anticipated to hinder or promote flow direction for groundwater.

An illustration of some of the mapped faults in the study area can be seen in Figure 2 together with an image of the folded shales outcropping along the N4 route towards Skilpadhek border gate (Figure 3). These small scale folds mirror the regional folding event that took place in the study area that have been alluded to by Dietvorst (1988).

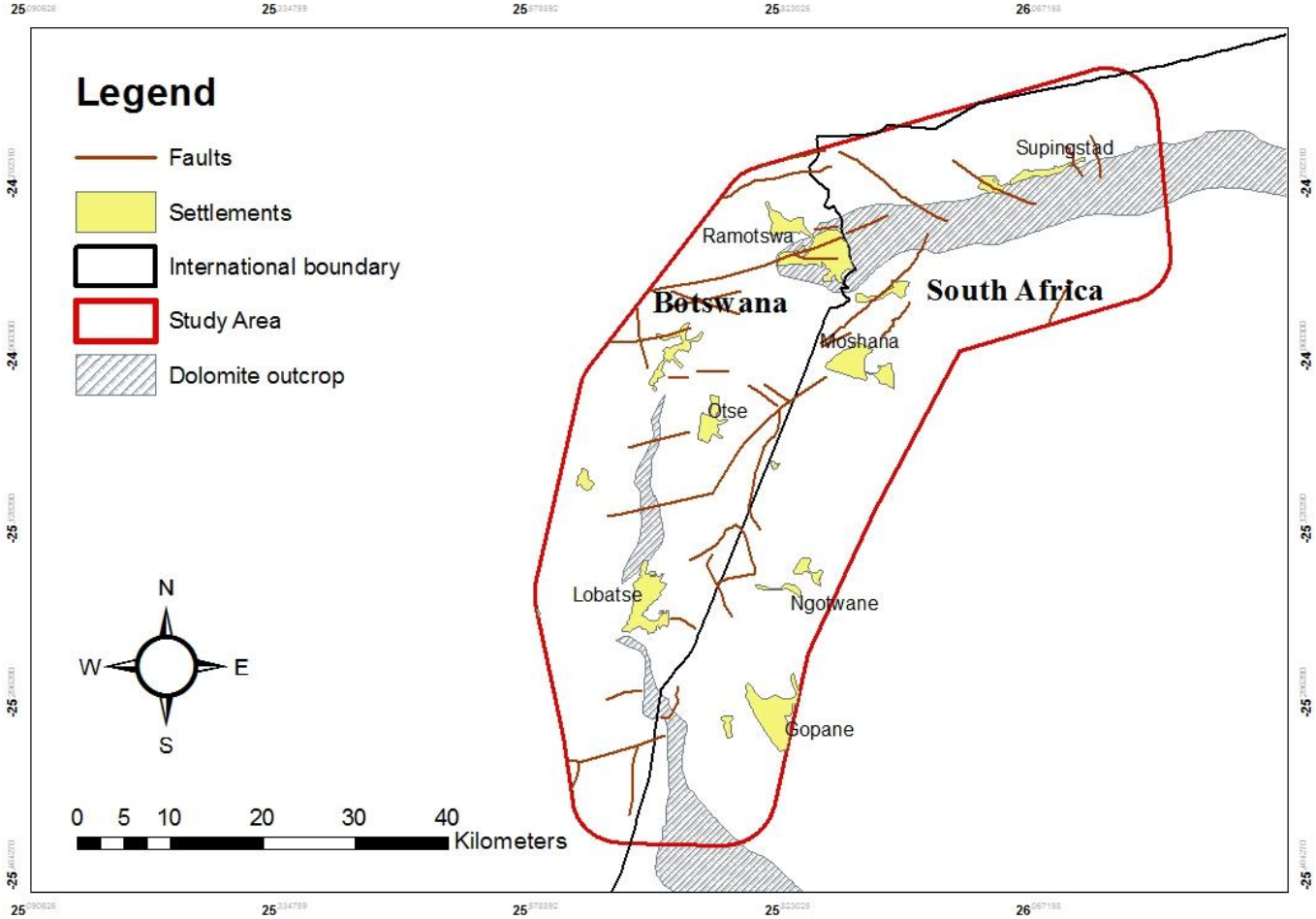

Figure 2. The orientation of faults within the study area (source: Council for Geoscience; Botswana Geoscience Institute).



Figure 3. Folded shale outcrop along the N4 route toward the Skilpadhek border, South Africa.

The Transvaal Supergroup was deposited on the Venterdorp Supergroup. The Ventersdorp Supergroup was deposited in an intricate rift system about 2.64 Ga. Burke *et al.* (1985) has recognized the following evidence as reasons to propose the environment, which the Ventersdorp Supergroup was deposited to be in a continental rift environment based on the following evidence: uneven basement topography, lateral facies variation, volcanic rocks with bimodal silica content and linear faulted basin margins.

2.4 The Transvaal Supergroup and lithostratigraphy

The Transvaal Supergroup includes one of the world's most well preserved stromatolites, earliest and unique carbonate platform sequences (Beukes, 1987). This Supergroup overlies the Archean basement, the Witwatersrand and Ventersdorp Supergroups and is an end Archaean/early Proterozoic succession. The Transvaal Supergroup is made up of the Chuniespoort, Pretoria and Rooiberg Groups with the Black Reef Quartzite ubiquitous at the bottom of the Transvaal Supergroup. The rocks of the Transvaal Supergroup are strongly faulted by steep normal faults with bedding planes dipping east towards the basin centre (Crockett, 1972). This 15 000 m Transvaal sequence of about 2 550 to 2 050 Ma (Mega-annum) is relatively undeformed and of low grade metamorphosed clastic, sedimentary and volcanic rocks (Eriksson *et al.*,1993).

2.4.1 Black Reef Formation

According to Clendenin (1988) the Black Reef Quartzite Formation represents a combined phase of both tectonic and thermal subsidence. Fluvial sedimentation followed by shallow-marine conditions are depositional settings suggested by Key (1983) for the black reef sandstones as an Epeiric Sea made its advance into the Kaapvaal Craton. Key (1983) identified ripple marks in the Black Reef Quartzite indicative of currents moving northeast to southwest.

2.4.2 Chuniespoort Group

The Chuniespoort Group, the correlated group name according to Eriksson *et al.* (1993) in Botswana is the Taupone Group, is made up of the Malmani Subgroup, which is overlain by the Penge Formation that is overlain unconformably by the Duitschland Formation. Emphasis in this study was placed on the South African geological nomenclature as opposed to the Botswana geological nomenclature.

Sedimentation in the basin was attributed to extensional tectonics of the early Proterozoic three stage rift system and the tectonics that influenced this rift sequence were directed from southwest to northeast excluding the pre-Pretoria series unconfirmity (Clendenin *et al.*, 1988). The three stage rift sequence was shortly terminated by a regional unconformity (Clendenin *et al*., 1988). Clendenin (1988) attributed the folding in the upper Chuniespoort Group carbonates to be indicative of an uplift event associated with pre-unconformity tectonics which were influenced by regional compression.

The Malmani Subgroup is of significant interest to this study because it hosts the Ramotswa Dolomitic Aquifer. A carbonate ramp depositional model was documented by Clendenin (1988) for the Malmani Subgroup which included supratidal, intertidal, subtidal and shallow basinal facies (Eriksson *et al*., 1993). The mudrocks, dolomites and interbedded cherts that comprise of the Malmani Subgroup signify epeiric marine deposits deposited over a great portion of the Kaapvaal craton (Eriksson *et al.*, 1993). The dolomites and interbedded chert outcrops seen within the study area are illustrated in Figure 4 below. The sedimentary sequence preserved in the rock record was developed by the north-northeast ward transgressions (Eriksson *et al.*, 1993).



Figure 4. Dolomite with interbedded chert dipping at 36˚ south east found in the south-western region of the study area, South Africa.

Eriksson and Truswell (1974) have segmented this subgroup into five formations based on their stromatolite morphology and particularly on its chert content. This subgroup is up to 2 000 m thick and begins above the Black Reef Formation with the chert-poor Oaktree Formation. Overlying the Oaktree Formation is a 300 – 500 m Monte Christo Formation which starts with an erosive breccia and continues with chert-rich dolomite platforms with stromatolites (Eriksson *et al.*, 2006). Following the Monte Christo Formation is the 100-200 m Lyttelton Formation of dolomites that are chert-poor and followed by about 600 m thick Eccles Formation of stromatolitic dolomites that are chert-rich (Eriksson *et al*., 2006). The Frisco Formation forms the last of the Malmani Subgroup overlying the Eccles Formation which is chert-poor and becomes shale rich towards the top (Eriksson *et al.*, 2006). A simplified lithostratigraphic column is shown in Table 1 below highlighting the Malmani Subgroup of the Chuniespoort Group, which compose the Ramotswa Aquifer. The names in brackets representing the corresponding lithostratigraphic naming convention used in Botswana.

Table 1. Simplified lithostratigraphic column of the study area modified from (Eriksson *et al.,* 1993; Eriksson *et al*., 1995; Meyer, 2014).

Age (Ga)	Thickness (m)	Supergroup	Group	Formation		Lithology
2.35		Transvaal	Pretoria (Segwagwa)	Timeball Hill (Lephala)		sandstone, shale
	10-150			Rooihoogte		Conglomerate, sandstone
Regional Unconformity						
		Transvaal	Chuniespoort (Taupone)	Duitchland		Carbonate, clastic rocks
~2.43				Penge		Banded ironstones
~2.55	~400			Malmani Subgroup (Ramotswa Dolomite)	Frisco	Dolomite
	~600				Eccles	Cherty Dolomite
	100-200				Lyttleton	Dolomite
	300-500				Monte Christo	Cherty Dolomite
					Oaktree	Dolomite
	25-30		Black Reef formation			Quartzite, sandstone, conglomerate

A harmonized geological map (Figure 5) of the study area across the boundaries of the two states shows the dolomitic sequence with an arc shaped morphology. This map made use of seventeen geologic units. The works of Eriksson *et al.* (1993) seen in Table 2 was used as a guide to link and separate some geological units from previous existing maps from both South Africa and Botswana to come up with a harmonized map we have below.

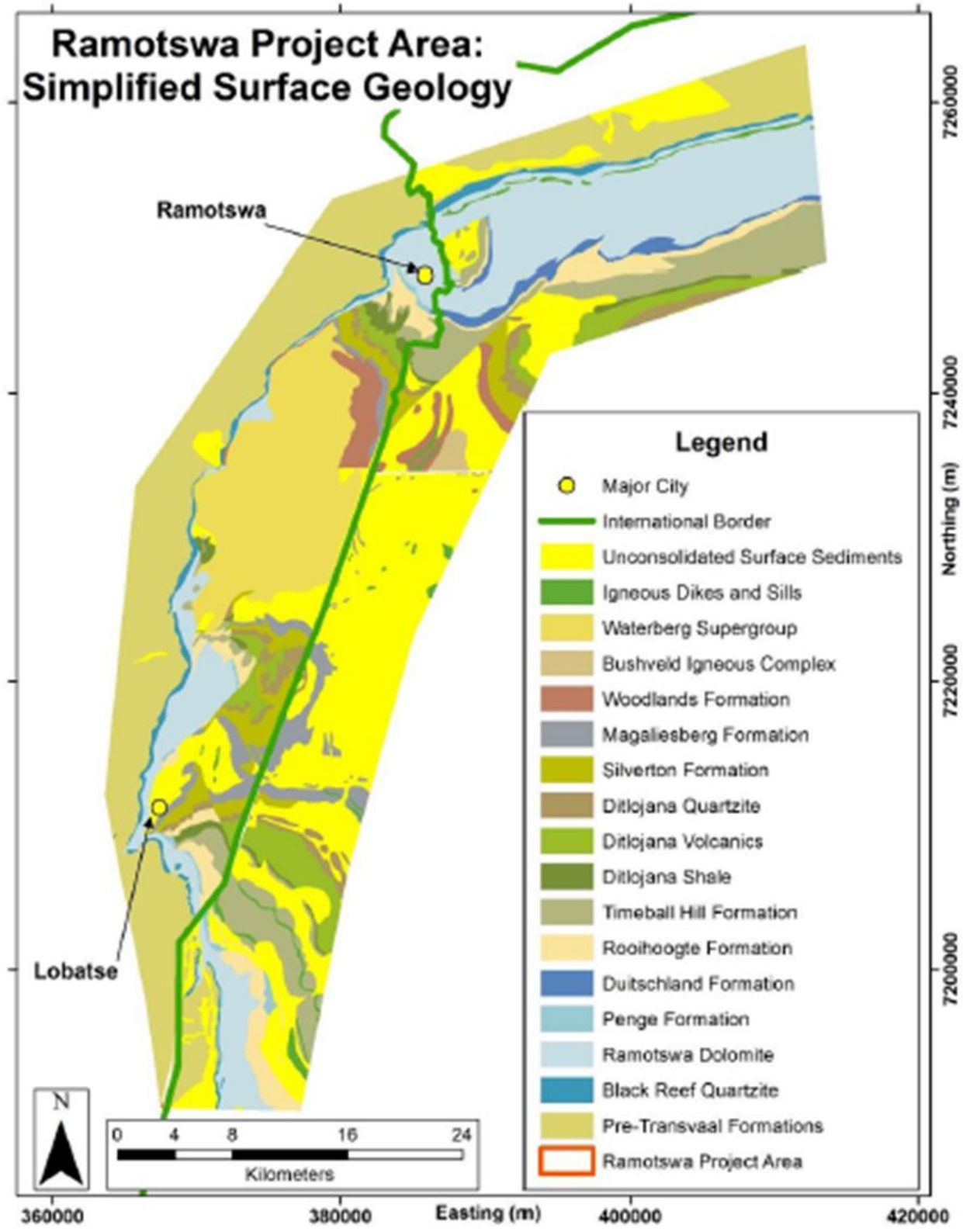

Figure 5. Simplified geological map of the study area (source: XRI Blue, 2016).

Table 2. Correlation of the Transvaal and Bushveld Basin in the South East District in Botswana and South Africa (modified from Eriksson *et al.*, 1993).

Overall Lithology	TRANSVAAL SEQUENCE (Transvaal or Bushveld Basin)			
	South East Botswana (Bushveld Basin)		South Africa (Transvaal Basin)	
Volcanics & clastic sedimentary unit			Loskop clastics & volcanics Damwal/Selonsriver Dullstroom lavas/ Smelterskop & Makeckaan clastics (lavas) Leeuwpoort sandstones	Rooiberg Group
Clastic sediments & volcanics	Woodlands volcanics		Rayton snadstones &shales &volcanics	Pretoria Group
	Sengoma sandstones		Magallesberg sandstones	
	Sengoma shales		Silverton shales	
	Ditlhojana sandstone/conglomerates		Daspoort sandstones	
			Strubenskop shales	
			Dwaalheuwel/Droogedal sandstones	
	Ditlhojana volcanics		Hekpoort andesite	
	Ditlhojana shales	conglomerates	Boshoek conglomerates/ sandstones	
		shales	shales	
	Tsokwane sandstones		Sandstone	Timeball Hill
	Lephala	shales	shales	
		Conglomerates/sandstones	Rooihoogte conglomerate /sandstones	
Regional unconformity				
Chemical sedimentary unit	Ramotswa shale		Duitschland carbonates, clastics Penge iron formations	Chuniespoort Group
	Magopane Maholobota Ramotswa	dolomites	Malmani dolomites	
Clastic sediments	Black Reef Formation		Black Reef Formation	
Clastic sediments & volcanics (Ventersdorp age)			Pre-Black Reef units – Wolberg Group & correlates	

2.5 Hydrogeological setting

There are two high yielding aquifer systems present in the study area, viz. the Ramotswa dolomite and the Lephala Formation. However, the Ramotswa aquifer dominates over a far greater area than the Lephala aquifer. Groundwater circulation in the dolomites is along the major linear karst feature orientated in an east-west direction (Staudt, 2003). Due to the mineralogical compositional differences of these two aquifers, karstification only develops in the Ramotswa dolomite.

The principal water bearing unit of the Ramotswa Aquifer, also known as the Ramotswa dolomite, corresponds to the Malmani dolomite lithostratigraphic unit within the Transvaal Supergroup. The aquifer has two zones of karst development according to (DWA, 2004):

(1) Upper karstic zone: varies in thickness between 20-50 m. Dissolution occurs along preferential fractures and the solution cavities are generally filled with secondary infillings
(2) Deeper karstic zone: varies in thickness of 25-50 m with open solution cavities

This dolomitic sequence is characterized by relatively high Mn and Fe and structurally forms part of the Transvaal/Bushveld basin (Martini and Kavaliers, 1976). This aquifer has been characterized as an arcuate of shallow to medium depth and being unconfined to semi-confined (Davies *et al.*, 2012).

The transmissivities of the aquifers are generally high (1170 m^2/day) with great storage and borehole yields (Staudt, 2003). This has been attributed to the chert-rich units of the Malmani subgroup, Eccles and Monte Christo Formations (Meyer, 2014). Dolomite and chert have different solubility's and consequently the reason we have more groundwater storage capacity in chert- rich dolomitic sequences than in chert-poor. Dissolution is supported in chert-rich units along bedding planes between dolomite and chert bands (Meyer, 2014). A summary of the two aquifers found in the study and its hydrogeological properties are tabled in Table3 below.

Table 3. Summary of the Aquifer's hydrogeological properties (Staudt, 2003).

Aquifer	**Lithology**	**Average Transmissivity (m^2/day)**	**Specific Capacity (l/s/m)**	**Storage Coefficient**
Ramotswa Dolomite	Dolomite	1170	2.7	5.7×10^{-2}
Lephala Formation	Shale and quartzite	492	3.5	8.7×10^{-4}

There are several ecosystem services that are dependent on the groundwater. On the South African side, the Ramotswa aquifer supplies domestic water to both urban and rural, used in agriculture for irrigation and livestock, and some spring water from these dolomites is let out into the environment (Pietersen *et al.*, 2011). On the Botswana side groundwater supply is used to supply the city of Gaborone and as a reserve for extremely dry periods.

2.5.1 Water levels and flow direction

Previous studies conducted in the study area were mainly from the Ramotswa wellfield and the Lobatse area, south of Ramotswa in Botswana. On the South African side, not much work had been done on water levels in the study area. Available data at time of the study showed water levels at different piezometers within the study recorded for different years. A hydrogeological environmental study by Beger (2001) in the Lobatse area found the groundwater levels with an average depth of about 17 m. Variation in these water levels was from 5 m to more 40 m (Beger, 2001).

The general groundwater flow direction reported by Staudt (2003) in the Ramotswa area was in a north-northeastern direction flowing the gradient and the Notwane river. In a study by Beger (2001) high groundwater levels were in the Lobatse area, in the south western region of this study, and groundwater flow is assumed to be in a north-easterly direction in the area.

2.6 Karst development

The Ramotswa transboundary aquifer is part of the regional karst system of the Malmani Dolomite. This karst system is unique compared to other classic karsts studied in the northern hemisphere. Holland *et al.* (2010) noted some features, which make the Malmani dolomitic karst system exceptional to be attributed to its lithologies that have been exposed to a variety of geological activities including folding, uplift, tectonisation and compaction due to deep burial. A significant distinguishing component of this karst is that it is subdivided into compartments which are isolated from each other by almost vertical dolerite and syenite dykes.

Karst refers to terrains underlain by limestone, or in the case of the RTAA, dolomite. The mineral composition of rock body is largely influenced to a great extent by its chemical

solubility and therefore, its hydrogeological properties (Goldscheider and Andrea, 2007). Carbonate rocks are karstifiable composed of calcite and dolomite. This study will focus specifically on dolomite, the mineralogical composition of Ramotswa aquifer.

Karst is generally regarded as the result of the solution of carbonate rocks. This is called karstification. When rain water interacts with the carbon dioxide in the atmosphere and in the soil, it forms a weak acid called carbonic acid (H_2CO_3). When this weak acid circulates through dolomitic rock ($MgCa(CO_3)_2$), it causes dissolution of the carbonate minerals. This leads to the formation of heterogenous conduit network and the chemical process is expressed by equation 1.

$$CaMg(CO_3)_2 + 2H_2CO_3 \rightarrow Ca(HCO_3)_2 + Mg(HCO_3)_2 \quad \textbf{(1)}$$

The dissolution process during karstification has been noted by Holland *et al.* (2010) as being more pronounced in the chert-rich units of the Malmani dolomite. This agrees with numerous authors who have attributed the Eccles and Monte Christo Formations to have under gone significant karstification, hence, its great capacity for groundwater storage. A distinguishing feature of a karst landscape is its underground drainage and landforms that evolve in response to precipitation and surface water flowing into the ground (IAH, 1999).

According to (Dreybrodt, 1988; Ford and Williams, 1989) karstifiability is controlled by three principal factors:

(1) Bulk mineralogical-chemical composition: Carbon dioxide controls the dissolution of carbonate minerals.
(2) Mineralological purity of the rock: Rocks with more than 25% impurities are generally regarded as not kastifiable.
(3) Degree of diagenetic compaction and cementation: This determines the hardness of the rock as well as its intergranular porosity.

2.6.1 Geomorphology

Four types of karst morphology have been identified by Martini and Kavaliers (1976) on the Malmani dolomites. These are the Plateau type, Escarpment type, Bushveld type and Vaal River type. Our study area comprises of two of the four identified karst morphologies and only these two will be elaborated:

(1) Plateau type: This marks the southern edge of the RTAA on the South African side and generally covers the Zeerust dolomites in the North West Province of South

Africa. This karst area is marked by flat plateau and the system is generally thought to be water-logged. Martini and Kavaliers (1976) seem to think that the plateau area karstification has not reached a mature stage.

(2) Bushveld type: The Transvaal dolomites reside in relatively low altitudes and form the northern border of the Transvaal basin. This type of morphology was seen on the Botswana side of the RTAA. Mature karst stage landform should be achieved by further evolution of its morphology.

2.6.2 Karst aquifer characteristics

Karst aquifers are significantly different from other hydrogeological environments and as such require specific investigation techniques. This is a result of dissolution and karstification of the carbonate rocks, which gives rise to its highly anisotropic properties. The following are some of the unique features common in karst aquifers:

(1) Evolution of karst aquifer may change with time as the infiltrating water containing carbon dioxide dissolves the carbonate rock. The orientation of the conduit network may change and collapse leading to unexpected groundwater flow paths. The aquifer's evolution is strongly related to flowing water (Goldscheider *et al.*, 2007).

(2) Spatial heterogeneity is common in karst aquifers due to its unpredictable conduit network.

(3) Karst aquifers are a special case as its hydraulic conductivity cannot be used to represent the entire aquifer system because of the effect of spatial heterogeneity. Hydraulic properties of karst aquifers are strongly controlled by large conduits or fractures (Goldscheider *et al.*, 2007).

(4) Duality of recharge and infiltration is a common phenomenon in karst aquifers. Recharge can be from the karst area (autogenic) or from an adjacent non-karst area (allogenic); and infiltrating water may originate from either point recharge features like swallow holes and or diffuse through overlying soils or through fissures (Figure 6)

(5) Flows in karst aquifer have double and even triple porosity. These are conduit flow, fissure/matrix flow and diffuse flow. A brilliant illustration of the heterogenous features common in karst aquifers is seen in Figure 6.

(6) Water table may rise or fall rapidly within a short space of time and the water quality may show variability with time. This is because karst aquifers are susceptible to temporal variability.

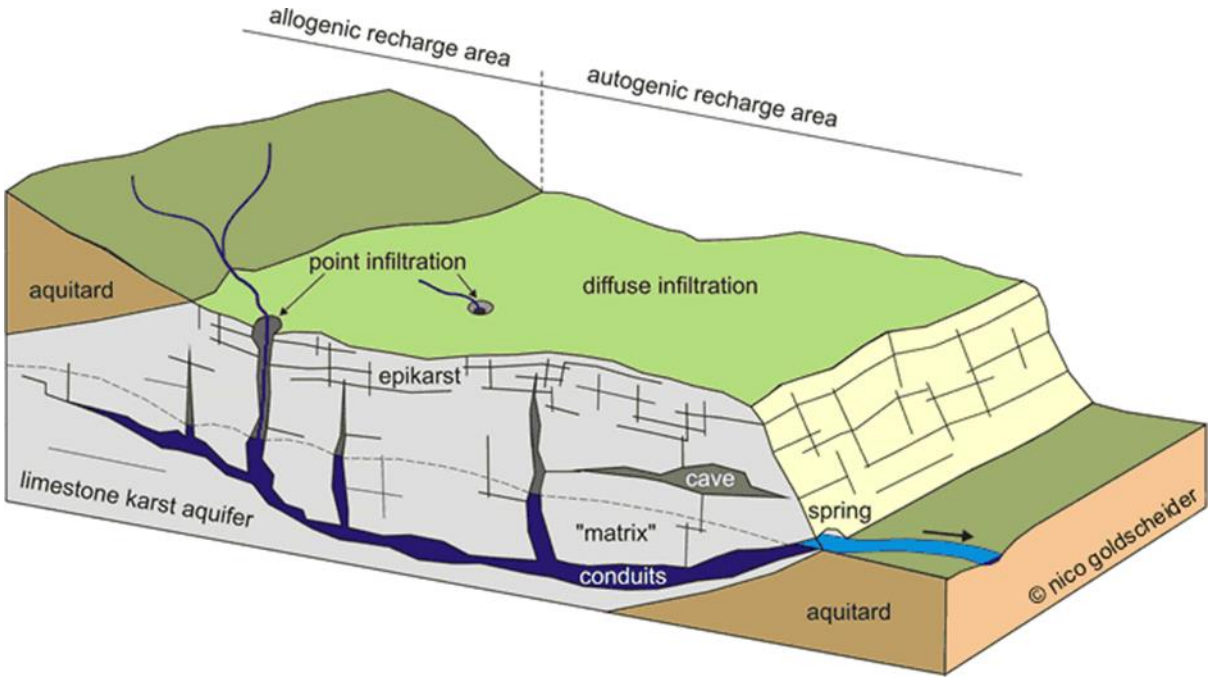

Figure 6. Diagram of a karst conceptual model illustrating duality of: recharge, infiltration and flow (Goldscheider *et al.*, 2007).

2.6.3 Compartmentalization of the Transvaal karst aquifer

The subdivision of the Malmani Dolomites into compartments make it a distinct type karst aquifer. These dolomites are compartmentalized by dyke intrusions of different ages, size and strike directions. The dyke intrusions are commonly prominent along NNW and E-W directions and are generally considered impermeable at depth and thus form barriers for horizontal groundwater flow (Meyer, 2014). Most springs have their position controlled by dykes, however, important springs such as the Dinokana spring, do not lead to cave systems as is the case with other karsts studied elsewhere in the world (Martini and Kavalieris, 1976). The Dinokana spring is a result of outflow against an impervious contact such as a fault or dolerite dyke and due to the thinning of the dolomite lithologies along the western outcrop on the South African side of the study area (Pietersen *et al.*, 2011)

Water level differences observed by Meyer (2014) across the compartment boundaries were noteworthy and based on this observation dykes were considered to be impermeable at depth while flow across boundaries took place in the upper weathered regions of the dyke.

2.7 Groundwater Pollution

Nitrate is a common groundwater pollutant with the increased concentrations being attributed to agricultural activities, influence from mines, animal waste, land use changes and sewage disposal (Kaçaroğlu and Günay, 1997; Stadler *et al.*, 2012). Although nitrate and nitrite are naturally occurring and form part of the nitrogen cycle, high concentrations of nitrate in the groundwater is concerning because it possesses serious health implications such as infant *methemoglobinemia* (a condition where nitrate is reduced to nitrite) and hypertension (WHO,1998; Wang *et al*., 2000).

Karstic groundwater is highly vulnerable to pollution. This is because pollutants enter the karst aquifers easily via thin soil layer and sinkholes. Pollutants are able to spread quickly and cover a large area within the karst aquifer as a result of the conduit network that allows for large volumes of water to flow. Natural attenuation processes are not as affective in karst aquifers compared to other aquifers making karst aquifers much more vulnerable to pollution (IAH,1999).

The Ramotswa wellfield located in the study area has had raised nitrate concentrations recorded in 1996 and the wellfield had to be decommissioned as a result (Ranganai *et al*., 2001). In the study by Staudt (2003) 11 boreholes were found to have exceeded the nitrate levels for drinking water by Botswana standard in the Ramotswa area with the maximum value of 442 mg/l recorded. The high nitrate concentration levels found in the groundwater was attributed to pit latrines and seepage from septic tanks (Ranganai *et al.*, 2001) and fractures in the upper karstic zone (Staudt, 2003). In the Ramotswa wellfield, nitrate concentrations are recorded annually and data available. However, there are no previous records of nitrate concentration data in boreholes on the South African side of the study. The Ramotswa wellfield continues to be a principal source of water for the city of Gaborone and the water is currently diluted with water supplies from elsewhere to bring down the nitrate levels to acceptable standards.

The vulnerability of an aquifer to pollution is normally caused by anthropogenic activities. According to Forster (1987) pollution is directly linked to the following factors:

(1) Method of pollutant disposition
(2) Physiochemical mobility and persistence of the pollutant
(3) Ease with which the mobile contaminants penetrate the saturated zone

(4) Physiochemical retention of pollutants due to natural attenuation

2.7.1 Environmental fate of nitrate

Nitrate and nitrite occur naturally and form part of the nitrogen cycle. In natural waters, nitrate is one of the main forms of dissolved nitrogen. Nitrate (NO_3^-) is the dominant and stable form in waters that contain dissolved oxygen and is highly mobile in groundwater with little or no retardation (Wang *et al*., 2000). Nitrite (NO_2^-) contains oxygen in an unstable state (WHO, 1998). According to Wang *et al.* (2000) dissolved nitrogen may be present in the following forms as: ammonium (NH_4^+), nitrite, nitrogen (N_2), nitrous oxide (N_2O) and organic nitrogen. The various processes of the nitrogen cycle are able to take nitrogen and covert it to the various nitrogen-containing compounds mentioned above. Organic nitrogen is converted to nitrate through the processes of ammonification and nitrification (Wang *et al*., 2000). The various processes and compounds involved in the nitrogen cycle in the environment and groundwater are illustrated in Figure 7. Nitrate may be lost from the groundwater system through the process of denitrification and conversely aerobic processes may result in accumulation of large quantities of nitrate in groundwater/soil (WHO, 1998; Wang *et al*., 2000). Several other factors that influence the fate of nitrate in the soil and or groundwater are but not limited to: the depth of the water table, amount of rainfall, soil type and presence of other organic material (Anuraga *et al*., 2006).

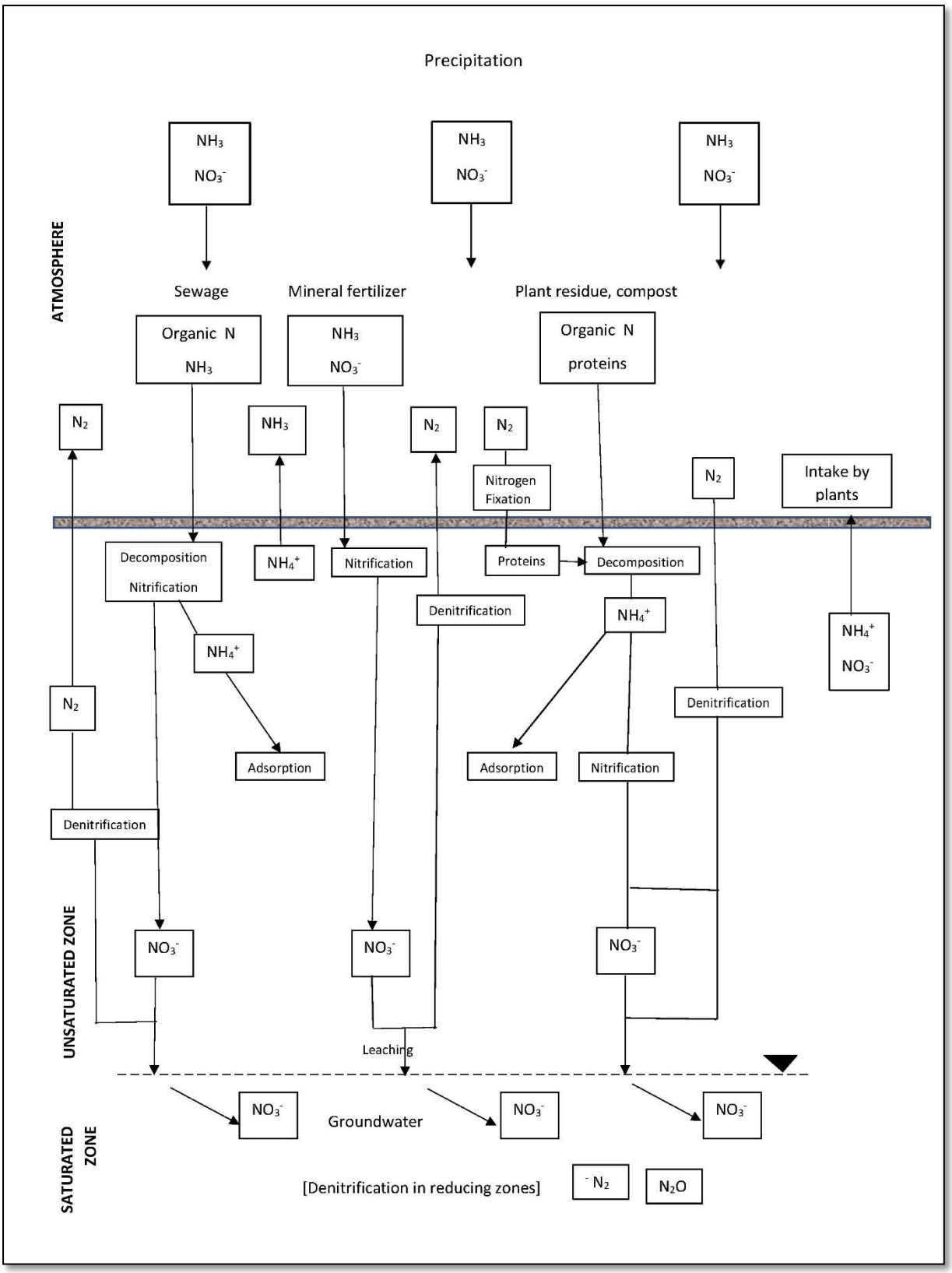

Figure 7. The fate of nitrate in the environment (Source: Staudt, 2003).

2.7.2 Drinking water quality standards

Generally, groundwater under aerobic condition has considerably low natural nitrate concentration of a few milligrams per litre (WHO, 1998). Due to public health concerns and the vulnerability of groundwater to pollution, a health based guideline value for nitrate in drinking water was set by the World Health Organization (WHO) and numerous countries have their own guideline values in place. The WHO guideline value for nitrate in drinking water is set at 50mg/l because, the majority of clinical cases of *mathaemoglobinaemia* being reported recorded nitrate levels greater than 50 mg/l (WHO, 1998). A comparison of nitrate guideline value for drinking water in Botswana and South Africa to the WHO guideline value are compared in Table 4.

Table 4. A comparison of nitrate guideline value for drinking water with country standards.

Guideline Parameter	**WHO (WHO,1998)**	**Botswana (BOBS, 2009)**	**South Africa (DWAF, 1996)**
Nitrate (NO_3^-) (mg/l)	50	50	20 (as total N)
Nitrite (NO_2^-) (mg/l)	3	3	20 (as total N)

3 STUDY AREA

The Ramotswa dolomitic aquifer was delineated by IGRAC (2012) as one of the 40 transboundary aquifers in Africa. The study area (Figure 8) is across two countries namely, Botswana and South Africa. In South Africa, the study area is part of the North West Province and more specifically in the Ramotshere Moiloa local municipality. In Botswana, the study area is located in the South East district.

The study area is referred to as the Ramotswa Tranboundary Aquifer Area (RTAA) after Altchenko *et al*. (2016). This study area corresponds with the fly zone where airborne geophysical survey was carried out in early 2016. However, a 5km buffer around this fly zone marks the boundary for this study which will also be referred to here as the RTAA.

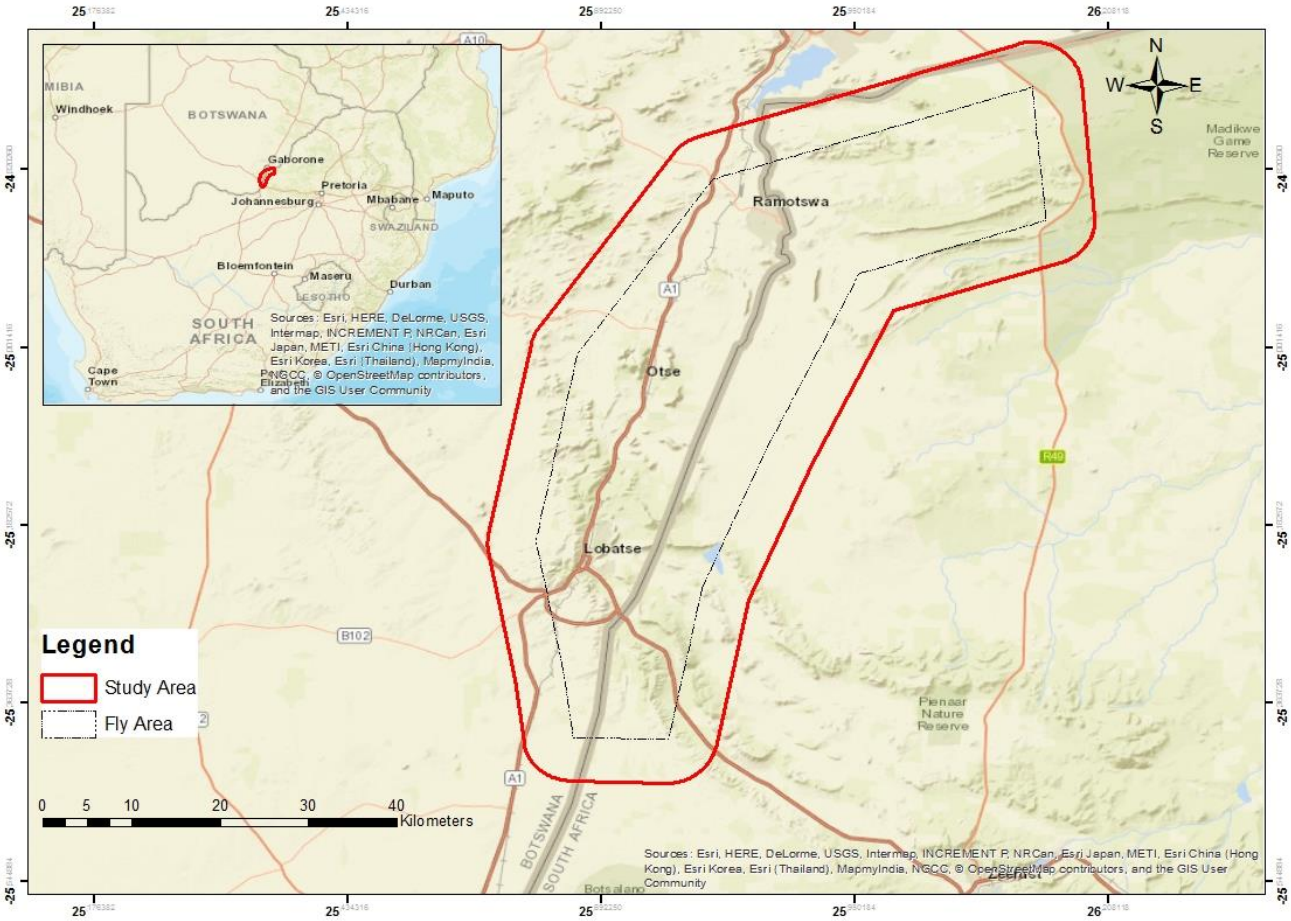

Figure 8. Location of the Ramotswa Transboundary Aquifer Area.

The study area covers settlements of Lobatse, Otse and Ramotswa in Botswana whereas in South Africa the study area comprises of Gopane, Ngotwane, Moshana and Supingstad villages, game reserves and agricultural farmlands. The population densities in districts or provinces in the study vary by over 50% difference with the population of 150 713 in Ramotshere Moiloa and 354 613 in the South East District (Statistics Botswana, 2011; Statistics SA, 2011). According to Statistics Botswana (2011) the population was highly concentrated in two villages in the South East district, with Ramotswa being one of these highly concentrated villages.

3.1.1 Water supply and sanitation

In the South East District majority of households have access to portable water with these water sources ranging from regional water schemes to borehole water. About 40% of the people in this district have access to flush toilets connected to sewage and about 20% have access to pit latrines (Statistics Botswana, 2011). Ramotswa has the highest use of pit latrines in the district at 11% (Statistics Botswana, 2011).

In Ramotshere Moiloa local municipality just over 70% of the people receive their water from regional/local water scheme while the rest obtain their water from boreholes, water tankers and other sources (Statistics SA, 2011). Almost 2% of the population in this district have a toilet connected to a sewage system and about 80% with unventilated pit latrines (Statistics SA, 2011). The comparison of the statistical data between the South East District and Ramotshere Moiloa local municipality need to be compared with caution as their population densities differ considerably.

3.1.2 Physiography

The Waterberg Supergroup rocks form some of the highest elevations in the study area forming an arc shaped ridges, the geometry visible on the digital elevation map (Figure 9). These shale outcrops dip at about 20˚ to a north easterly direction and are visible on the N4 road towards the Skilpadhek border in South Africa. The ridge features, also referred to as the western plateau by Key (1983), are of high elevation of about 1 334 m above sea level (mamsl) drain in the easterly or north easterly direction by the Notwane river system which is found at lower topographic elevations of about 1 025 m above sea level in the study.

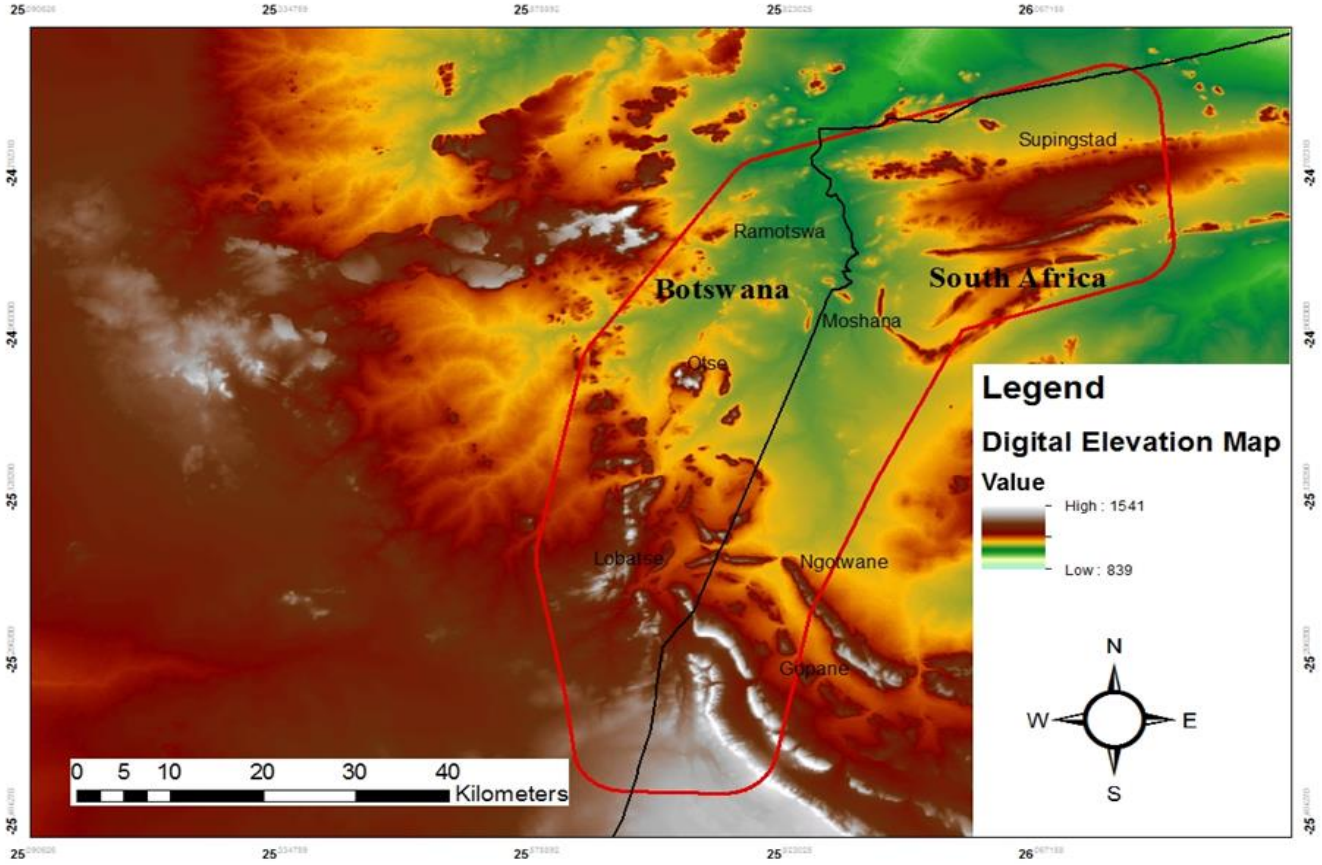

Figure 9. Digital elevation map for the study area, indicating the highest and lowest elevation at about 1 334 mamsl and 1 025 mamsl respectively.

3.1.1 Climate

The study area lies in a semi-arid climatic setting known for its warm summers and cool dry winter seasons. This is strongly influenced by the southern hemisphere weather patterns, which comprise of two seasons: Summer (October to March) where rainfall predominates and Winter (April to September) with little to no rainfall. Extreme rainfall events with high intensity over a short period are common in this region. One such event was the recent flooding of the Notwane River in March 2016 which recorded 105 mm of rain overnight in Ramotswa (Mpaetona, 2016).

The mean annual precipitation (MAP) over the study area between 1995 and 2005 is at maximum in the eastern part with 547mm and decreases towards the western side with an MAP of 472mm in Lobatse. The positions of the rainfall stations within and around the study area are indicated in Figure 10. Altchenko *et al.* (2016) cautions against the values of annual rainfall values of stations in South Africa attributed to missing values for some year.

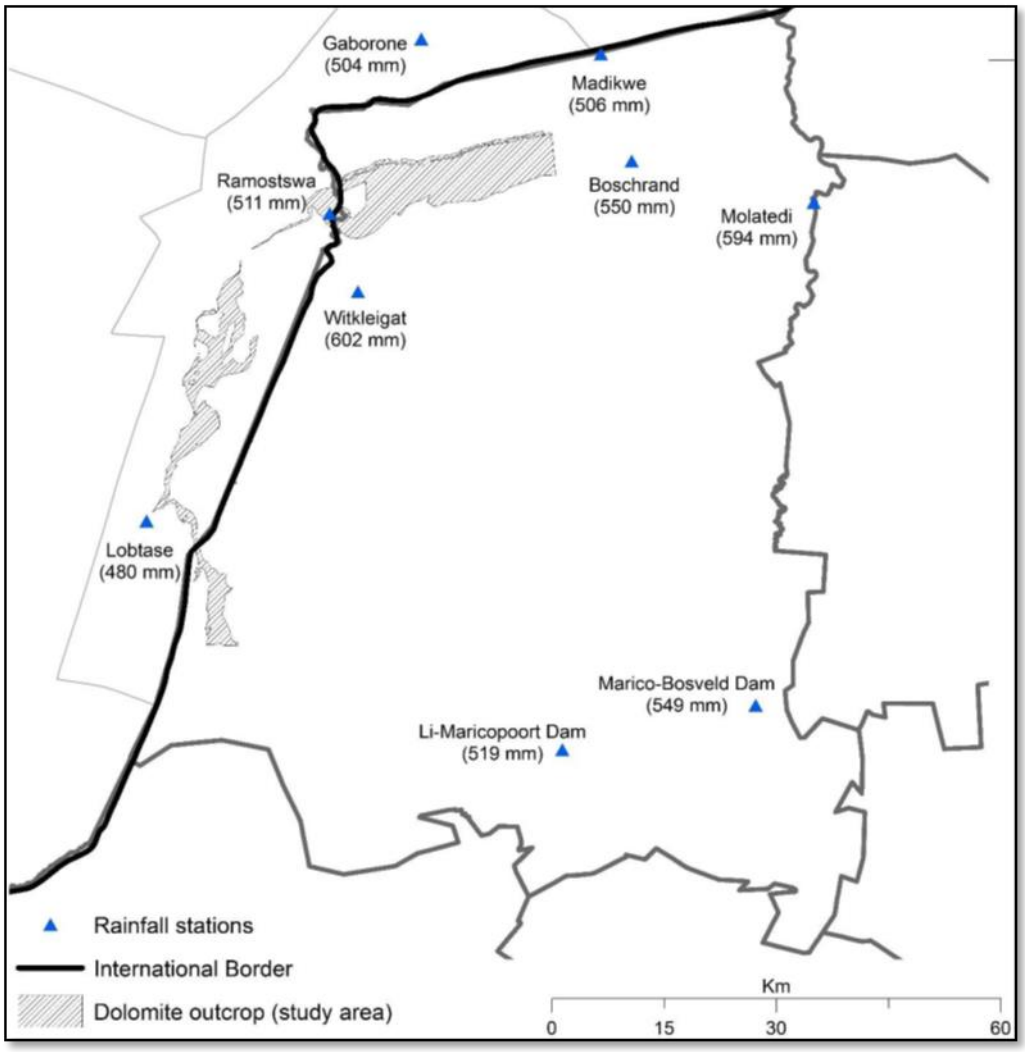

Figure 10. Position of the rainfall stations in and around study area (Altchenko *et al*., 2016).

A comparison of the monthly rainfall values between the weather stations in Botswana and South Africa in and around the study area appear to have a similar rainfall pattern. The pattern illustrated in Figure 11 confirms the summer rainfall months between October and March with significant rainfall occurring in the month of January.

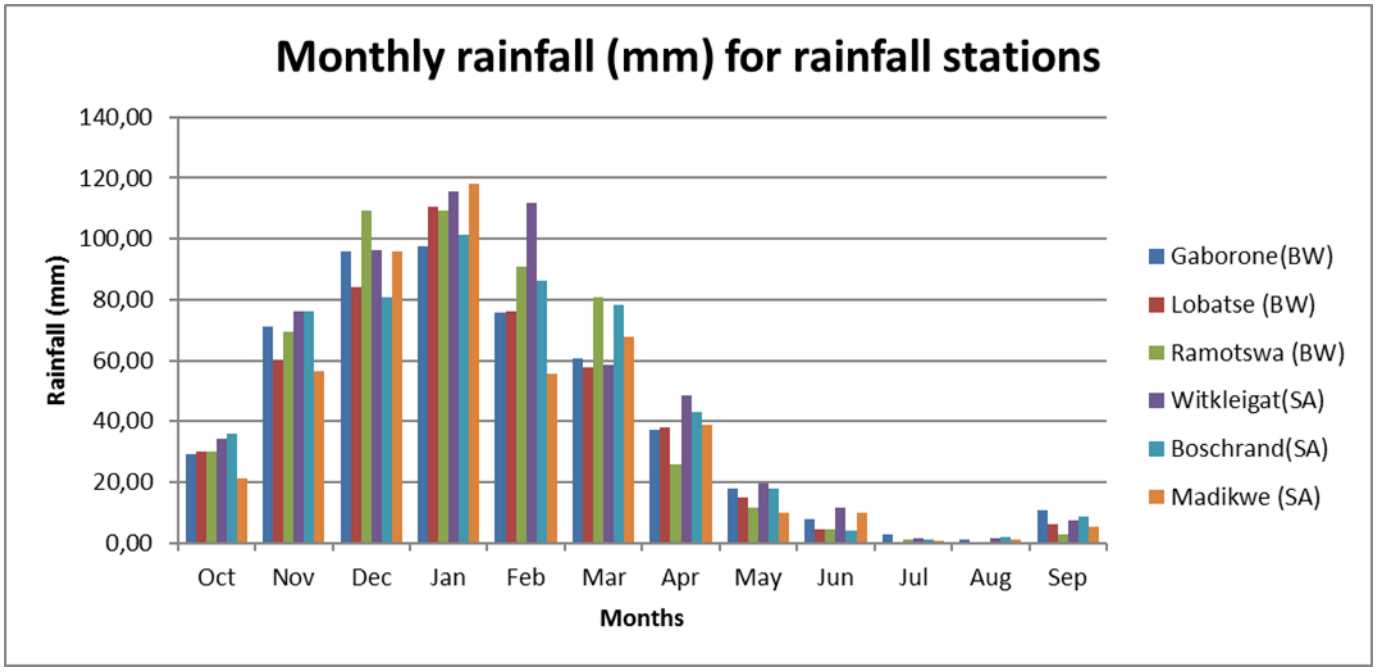

Figure 11. Comparison of monthly rainfall across rainfall stations (Source: Altchenko *et al.*, 2016).

3.1.2 Sub-catchments of the Limpopo River Basin system

Ramotswa aquifer forms part of the Limpopo River Basin system located within the Notwane and Marico sub-catchments. Notwane (Figure 12) is the principal sub-catchment in which the study is located and feeds into the upper confluence of the Limpopo River (FAO, 2004). Notwane River is one of the main tributaries of the Limpopo River Basin and flows in a northeasterly direction up until it reaches the Limpopo River and Marico River. Key dams (Gaborone and Bakaa) for domestic water supply to the city of Gaborone and neighbouring settlements are located on the Notwane River.

The Notwane catchment area is about 18 053 km^2 with a mean annual precipitation of between 450-500 mm and mean annual evaporation of 1 950 mm (FAO, 2004). This sub catchment constitutes 4.4% of the entire Limpopo River Basin.

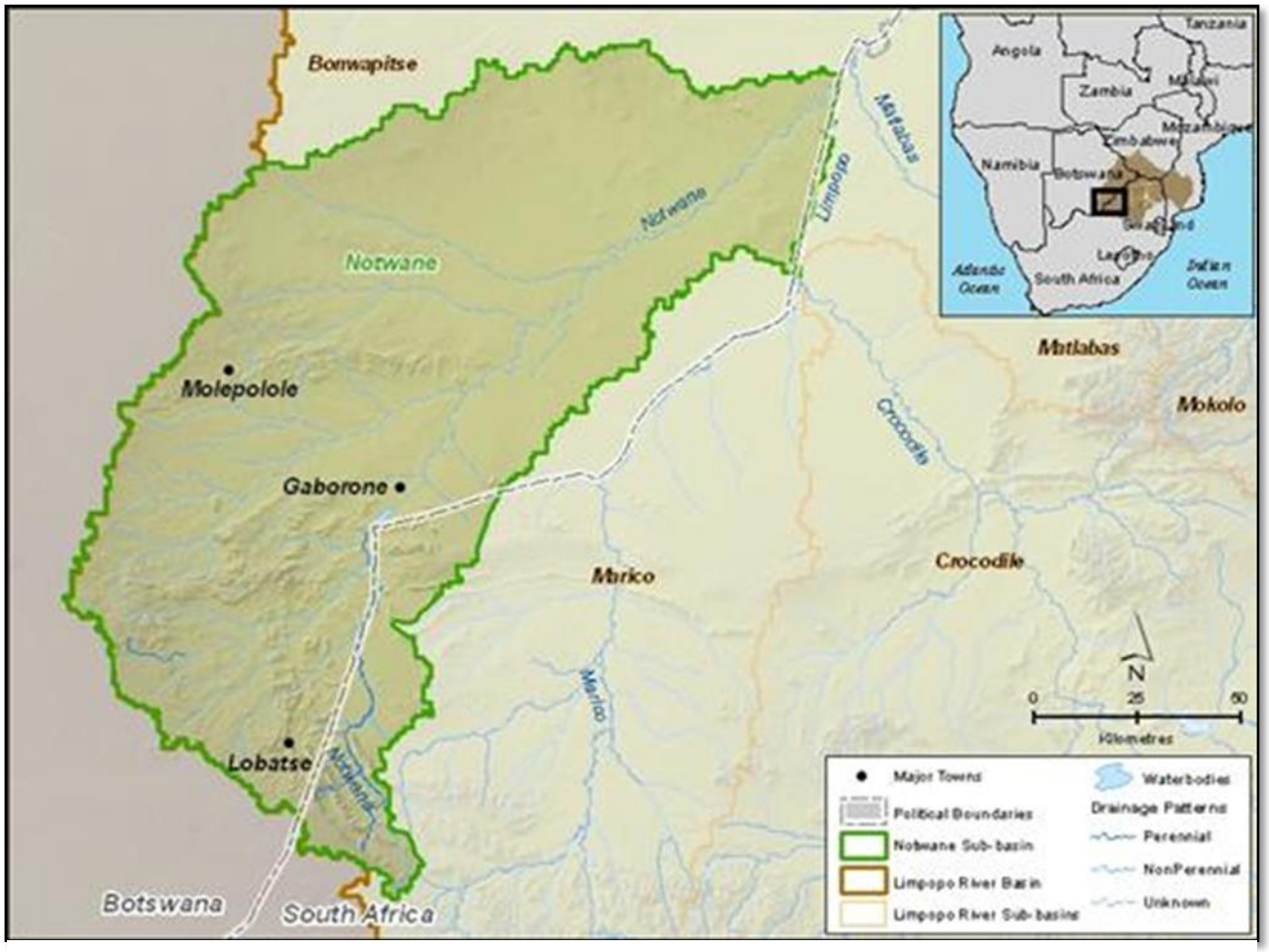

Figure 12. Notwane catchment within the Limpopo River Basin

(Source: http//www.limpopo.riverawaenesskit.org/).

3.1.3 Dinokana Spring

The perennial Dinokana spring (Dinokana upper) is found within the Ngotwane catchment. This spring forms in one of the Chuniespoort Group dolomite compartments. According to Meyer (2014) Dinokana spring is located within the Dinokana compartment, which has an area of 277 km^2. The mean spring flow in 2008 was 3.6 Mm^3/annum (Meyer, 2014). The Dinokana spring flow record between 1990 and 2015 is displayed in Figure 13 below.

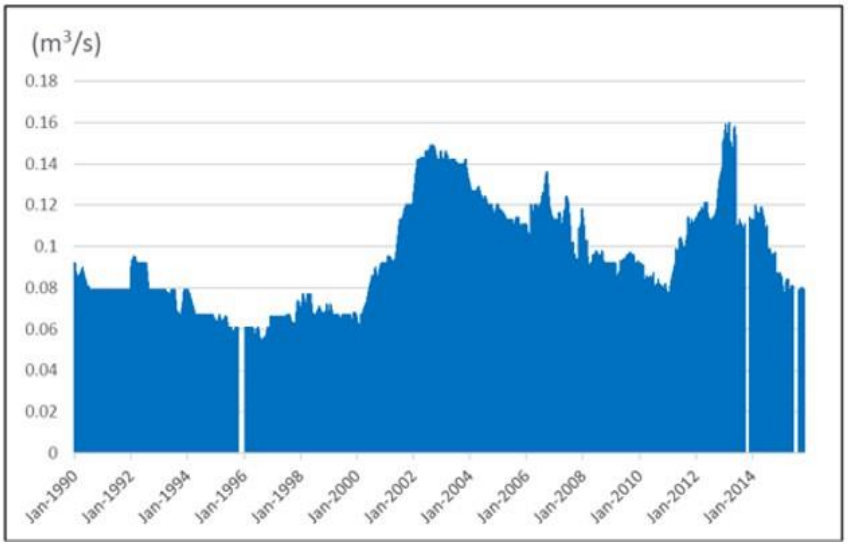

Figure 13. Dinokana upper eye flow record 1990 - 2015 (Altchenko *et al.*, 2016).

4 METHODOLOGY

4.1 Data sources

A collaborative effort between the Department of Water and Sanitation of South Africa and Department of Water Affairs, Botswana, facilitated by International Water Management Institute (IWMI) made data available from both states for this study.

The Department of Water and Sanitation of South Africa conducted water level measurements in 2016 in the Ramotshere Moiloa Local Municipality particularly in current study area. The data was obtained directly from the Department of Water and Sanitation in North West Province. A few water level data were obtained from HYDRA datasets. In Botswana, water level readings were measured with the support of the Water Utilities Corporation technical team. Dinokana spring long term daily water flow time series data was obtained from the Department of Water and Sanitation hydrological services website (http://www.dwa.gov.za/Hydrology/).

Geological maps were obtained from the Council for Geoscience South Africa and Botswana Geoscience Institute (formerly known as Department of Geological Survey Botswana). Hard copies, soft copies and shapefiles were also provided by these departments. XRI Blue Company was commissioned by IWMI to create a harmonized geological map along the international boundary of South Africa and Botswana for the project area.

4.2 Sampling sites

The borehole/piezometer sampling sites within and on the periphery of the study area were selected based on the following criteria in order of importance:

(1) Lithology that the borehole intersect was dolomite, this was to ascertain that the water level measurements and other field parameters are that of the Ramotswa dolomitic aquifer.

(2) Physical accessibility to the borehole site for water sampling.

(3) Accessibility to the borehole water for groundwater samples and in situ field parameters.

Sampling sites (Figure 14) were selected with the aim of representing the entire study area. However, the position of pre-existing boreholes/piezometer used for the study and the criteria mention above limited coverage within the study area.

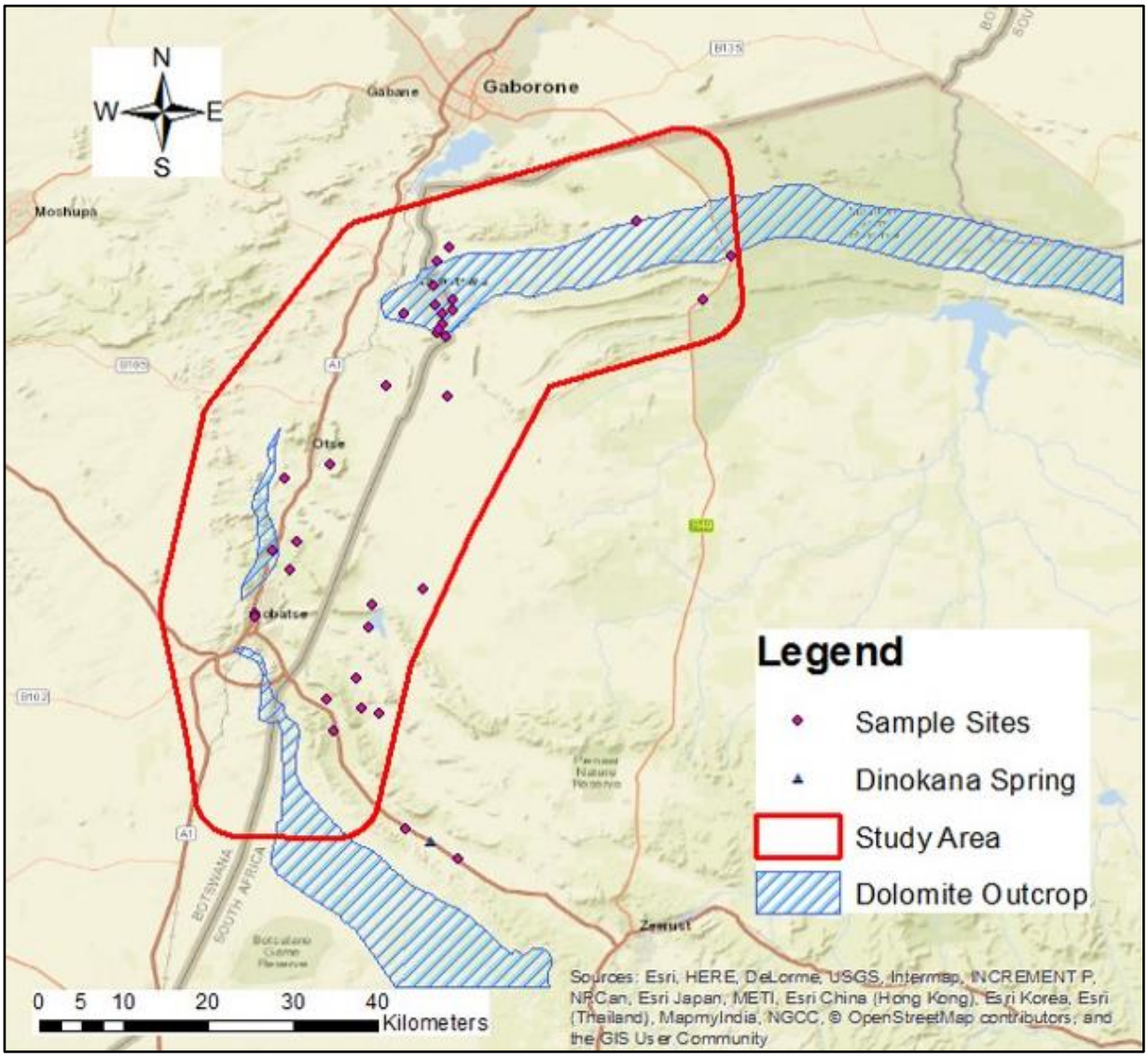

Figure 14. Sample location for water quality analysis.

4.3 Water level measurement

Water level readings from the piezometers were conducted using a dip meter. Water level was measured by taking a reading directly from the tape at the top of the borehole casing. The casing collar height above the ground was subtracted from water level measured in metres below ground level (mbgl), whereas data acquired from Department of Water and Sanitation was already given in mbgl units. The water level readings were taken during the cool dry winter months of July and August 2016 in both Botswana and South Africa.

The final depth to groundwater level was calculated using Equation 2.

$$\text{Groundwater level} = A_{surface} - D_{groundwater} + H_{casing} \quad \textbf{(2)}$$

$A_{surface}$: Altitude above mean sea level of ground surface (m)

$D_{groundwater}$: Depth of groundwater level from upper end of borehole casing (m)

$H_{casing:}$ Height of casing collar above the ground surface (m)

4.4 Piezometric map construction

Due to insufficient piezometric water level data measurements across the study area measured within the same year or season. It was difficult construct a piezometric map for the study area, particularly on the South African side of the study area. However collaborative efforts together with the Department of Water and Sanitation ensured that water levels for piezometers/boreholes covering the study area were measured in 2016.

The groundwater levels from the various piezometers for the year 2016 were put into Arc GIS for the construction of a piezometric map. This software makes use of a geostatistical procedure called kriging. This procedure assumes that the distance between sample points mirrors a spatial correlation that can be used to explain variation in surface. The procedure is most suitable when there is a spatially correlated distance or directional bias in the data. The method was applied to the dolomitic aquifer because it was inexpensive and readily available method that does not require costly site specific data.

4.5 Groundwater sampling

In order to obtain groundwater samples representative of the aquifer, bore purging was performed at the sample sites in Botswana. Purging allows for the removal of the stagnant water in the bore casing. Well purging was performed with the *Grundfos* SQ 1.2 – 3N (76.2 mm diameter) submersible pump fitted with a Teflon sampling lines (Figure 15). The groundwater was purged for a minimum of 40 minutes and a maximum of 60 minutes. Phyiso-chemical analysis was performed on site at 10 minute intervals, to check for the consistency in measured parameters, to maximum purging time.



Figure 15. Well purging after uncapping the borehole.

Each site was sampled once for nitrate and nitrite analysis and for microbiological indicators. A total of 36 groundwater samples were taken from the study area. 18 of the groundwater samples were collected from the Botswana side, the other 18 groundwater samples collected from the South African side. Standard groundwater sampling practices documented by Weaver *et al.* (2007) were employed.

The Botswana groundwater samples were obtained from observation, production and private boreholes. The South Africa groundwater samples were obtained from private boreholes and from windmill pumped boreholes for livestock watering. Access to Department of Water and Sanitation boreholes was sealed off, hence the alternative groundwater sample sites used.

4.6 Analytical Methods

Hydrochemical analysis was used to determine amount of nitrate and nitrite concentrations in the groundwater samples while, microbiological analysis is used to delineate nitrate pollution source. Samples for each site were made up of 500 ml sample for nitrate and nitrite analysis and 500 ml groundwater sample for microbiological analysis in a

disinfected or glass bottles. The samples were immediately chilled with ice (4˚ C) in a cooler box and transported to the laboratory within 24 hours of collection.

Samples were sent to Resource Quality Information Services (RQIS) laboratory – Department of Water and Sanitation in South Africa and Water Utilities Corporation (WUC) laboratories in Botswana. Hydrochemical analysis performed by both laboratories used continuous flow spectrometric method for the determination of nitrate, nitrite or the sum of both.

Microbiological analysis was performed using different methods by the laboratory in Botswana and South Africa. At RQIS laboratory, the Colilert method is used to determine of both total coliform and *Escherichia coli* (*E. Coli*) numbers. At the WUC and Aspirata laboratory, total coliform and *E. Coli* counts were made using a filtration method using agar (Brilliance *E. Coli*/Coliform Agar). These two methods are significantly different in that the former method is a statistical probability of the number of organisms per 100 ml based on the number of dilution tubes that grew, whereas the latter is an actual total count of colony forming units from the surface of the plate. For this reason, the study will take a much more generalized approach when comparing the total coliform and *E. Coli* numbers analyzed by the different laboratories across the entire study area.

4.7 Microbiological investigation

Total coliform and *E. Coli* were chosen for microbiological analysis for water quality study. These coliform organisms have been used by several researchers (Lewis *et al.,* 1978; and Cimenti *et al.,* 2005) as indication of fecal pollution and to predict presence of pathogenic microbes. This method was used together with physical knowledge of the surrounding environment to trace to source attribution of nitrate pollution of the groundwater. Microbiological investigations were much easier and less expensive to perform as opposed to nitrate isotope investigations.

E. Coli was used as an indicator of fecal pollution and because its present at greater concentrations than the pathogens it predicts (Scott *et al.,* 2002). Total coliform provides indication of other disease causing organisms in the water body and was much easier to be picked up in a laboratory since its life span outside the warm-blooded animals does not deteriorate as drastically as *E. Coil* (Lewis *et al.,* 1978). These microbial indicators have been beneficial in protecting human health and have been used to warn us but, they have limitations. These microbial indicators lack specifity to discriminate between human and

animal pollutant sources. This was why this method is coupled with knowledge of the surrounding environment to allow for a better determination of the source of nitrate pollution.

4.8 Quality assurance and Control

To detect variability related with laboratory analysis, quality assurance and quality control procedures were used. Two sets of samples (BH4450 and BH310) were collected at two sample locations which were sent to two laboratories: WUC laboratory and RQIS laboratory. A comparison was made on the hydrochemical analyses results performed by both laboratories on the same samples. The purpose was to assess the variation in sample analysis by the different laboratories and if there was any similarity in the laboratories findings.

4.9 Physio-chemical analysis

Field parameters were measured on site for temperature, pH, Electrical Conductivity (EC) and Total Dissolved Solids (TDS) using OXI 4SP Crison. The meter was calibrated using two buffer solutions, pH 4 and pH 7. For the purged boreholes, the field parameters were recorded several times at ten minute intervals until the maximum purging time had lapsed. This was to try get a more stabilized reading that will confirm that the actual groundwater source was actually being measured.

4.10 Identification of potential groundwater pollutants

At each sampling site a thorough inventory of the surrounding and borehole location was recorded together with the potential pollution sources and land use types. A sketch of the well and surrounding environment was also recorded. This inventory takes stock of the following specific categories available in the appendix A:

- Primary use of well: Community/ Observation/Production/Domestic use
- Well design: Covered or not covered/ Fenced
- Land use: Urban/Rural/Natural/Agriculture/Other
- Potential pollution sources: Septic tank/pit latrines/fertilized fields/ non-visible or other
- Domestic waste system: Septic tank/ Sewer system/pit latrines/other

4.11 Nitrate pollution map

One of the main objectives of this study was to produce a map of the study area indicating the spatial distribution of nitrate. The map will give an indication of the extent of groundwater pollution and or vulnerability in the study area. This map was produced using ArcGIS software.

4.12 Airborne Electromagnetic (AEM) data acquisition and interpretation

Helicopter-borne Time Domain Electromagnetic (TDEM) surveys was carried out by Exploration Resources International (XRI) over the study area indicted in Figure 8 as the fly zone. TDEM offers a wide variety of effective sounding depths from 6 to 900 m (Bechtel *et al.*, 2007).

Electrical properties of the earth's land surface material were characterized using electromagnetic induction which provides airborne electromagnetic (AEM) data. In order to collect this data a transmitter coil sends an electrical current through a big loop of wire made up of multiple turns which generate an electromagnetic field. Once this electromagnetic (EM) field is stable, the transmitter coil is switched off and EM field begins to dissipate and decay into the subsurface. The dissipation rate is controlled by the electrical properties of the subsurface. The subsurface generates a decaying secondary EM field which is induced when the transmitter coil is shut off creating a current in the receiver coil. This current is measured at different time gates. The sounding curves are numerically inverted to create subsurface resistivity with depth (XRI Blue, 2016).

The AEM data in the study area is acquired using the SkyTEM 508 (Figure 16) airborne electromagnetic system. The 508 is a firm frame, dual magnetic moment transient airborne electromagnetic (TEM) system. The processed and inverted AEM data was then interpreted geologically by XRI.

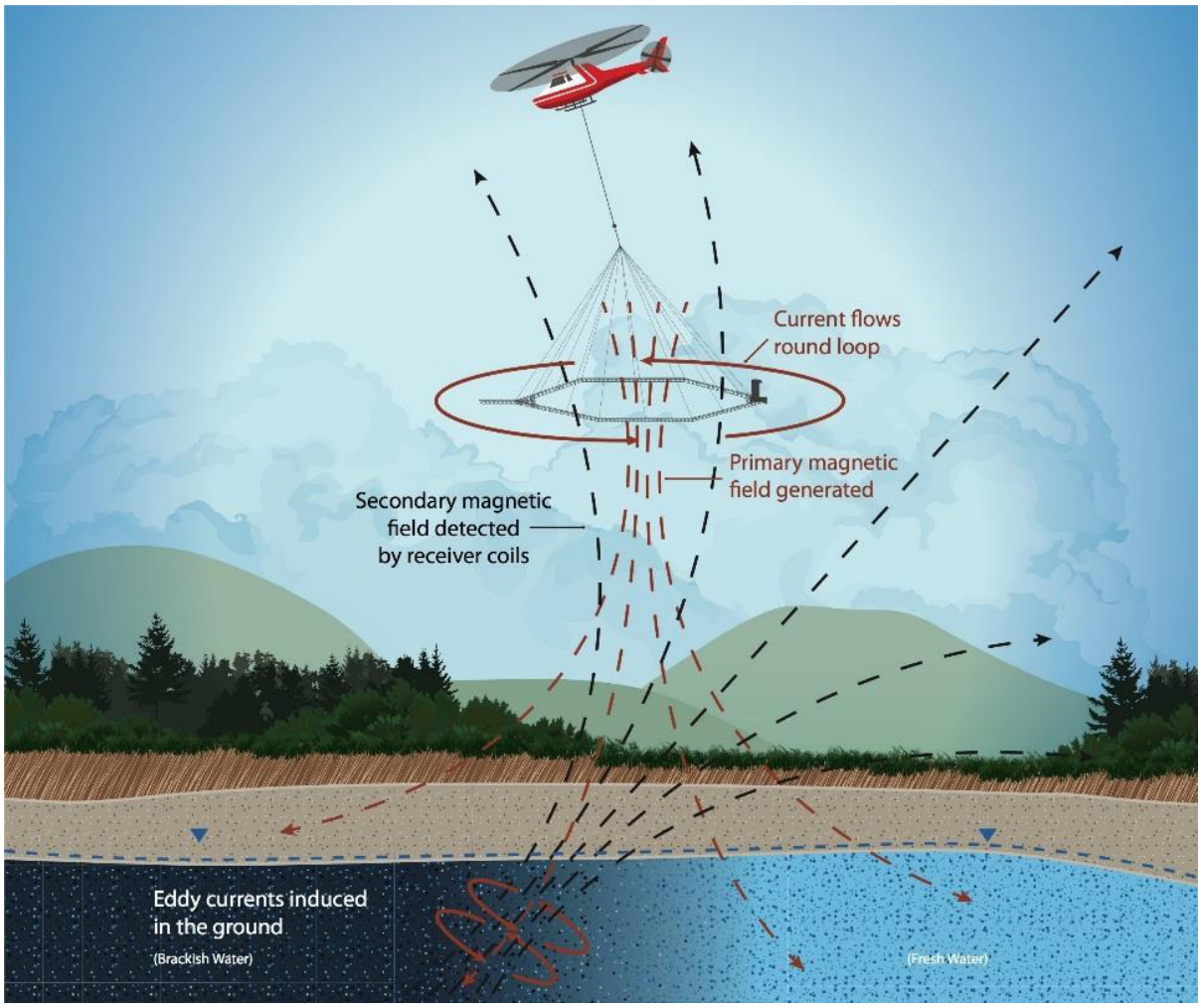

Figure 16. Illustration of an airborne electromagnetic survey (source: XRI Blue, 2016).

SkyTEM is particularly useful in karst hydrogeology in determining the depth and thickness over burden, intrusions such as dykes, detection of collapsed features and depth of water table. This was useful in characterizing some components of the aquifer. The advantage of using dual moment is obtaining both shallow resolution and deep resolution of the subsurface. However, the method is prone to interference from metal structures and power lines and not applicable in built-up areas (XRI Blue, 2016).

4.13 Spring hydrograph analysis using RECESS program

Springs provide both measurable and visual indication of the response of groundwater to rainfall. In the study Dinokana spring, which forms part of the Malmani dolomites in the Zeerust area, was investigated. The evaluation of this spring gives a broader evaluation of the aquifer properties and even estimate the discharge sustainability.

A computer program called RECESS was used to estimate the recession index from the spring discharge records. This approach was inexpensive and relies on spring discharge data, which is available for free. The method does not require drilling activities which are highly expensive and require a lot of money which developing countries such as South Africa and Botswana often cannot spare. The RECESS program provides input values used in a program called CURV. This program shows the solutions to the MRC without showing each segment (Rutledge, 2007).

4.13.1 Description of the method

The RECESS program makes use of an empirical method to calculate a best fit linear equation to obtain MRC and Recession index (K). The program identifies periods of continuous recession and the program user selects segments that represent near linear conditions which, are used to quantify the recession index (Rutledge, 2007). Once segments have been selected the program calculates a mathematical expression given in Equation 3.

$$t = K_1 \times \text{Log } Q + K_2 \qquad \textbf{(3)}$$

Where, t: time (days)

LogQ: logarithm of flow

K_1 & K_2: coefficients derived from linear regression.

The program then uses Equation 3 to derive recession index (days/ log cycle). Once all the recession segments within selected period are identified, calculations to determine expression for MRC can now be performed. The program derives a best fit linear equation for K as a function of Log Q, represented by the straight line seen in frame B in Figure 17 (Rutledge, 2007). In Equation 4, t is the time and A, B, C represent coefficients of the polynomial equation which are used to derive MRC (Rutledge, 2007).

$$t = A \times (\text{Log } Q)^2 + B \times (\text{Log } Q) + C \qquad \textbf{(4)}$$

The schematic representation of procedure used to obtain MRC is shown in Figure 17. The MRC is an integration of best fit linear equation for K as a function of Log Q (Rutledge, 2007). This method assumes a linear relationship between K and Log Q. An ancillary program called CURV is then used to extract the solution for the MRC equation combining all the individual segments. MRC is used to counter variation in recession curves from different years, hence the MRC technique is used to construct a mean recession curve.

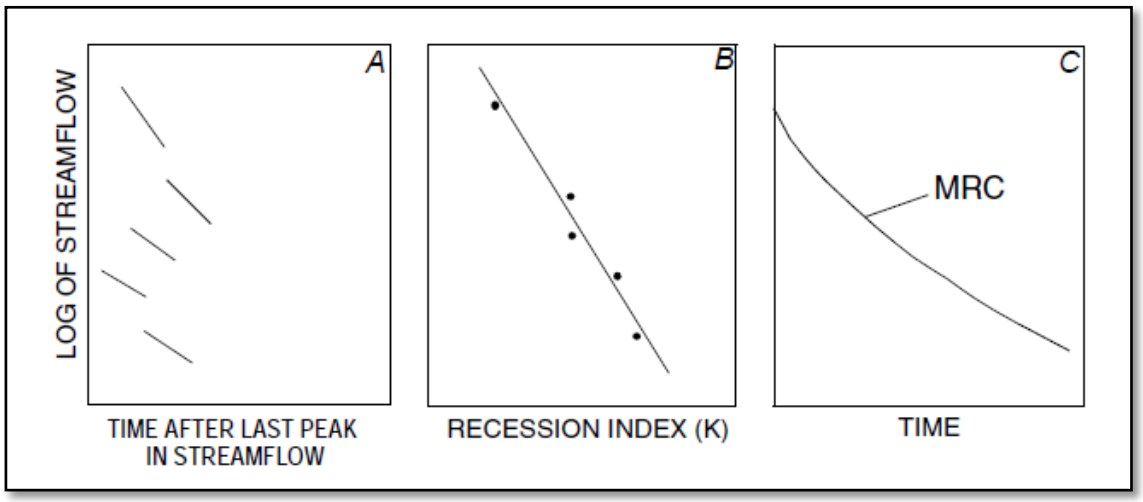

Figure 17. Methods used to determine the master recession curve (MRC): (A) Selected recession segments, (B) Recession index (K) and best fit line (C) Master Recession Curve derived from coefficients in B (Rutledge, 2007).

4.13.2 Determination of Recession Index (K) and Master Recession Curve (MRC)

The recession index (K) was estimated using RECESS program with the Dinokana spring discharge data. Recession index characterizes the combined groundwater response and used as a substitute for overall groundwater storage conditions (Kienzle, 2006). The recession index can be used to predict the expected spring discharge response in the coming months and years (Kienzle, 2006). Daily spring discharge data from 1990-2015 were considered as the model input data to produce median recession index and a MRC for the Notwane catchment area. The data was not divided into any particular season. The CURV program generates 50 values of recession segments analyzed in the RECESS program. These values of Log of flow and time are plotted in the R.C 4.0 tool to generate a master recession curve. The master recession curve reflects the general characteristics of the watershed area where the spring is located (Kienzle, 2006). The construction of a mean MRC tries to overcome the problem of time variability in recessions (Tallaksen, 1995).

There are several simplifications associated with the method discussed above. The linear recession model used was a reasonable approximation. The method assumes the absence of evaporation and limit periods for departures from linearity was assumed to be 7 and 15 days for each recession period, which was a fair assumption for the semi-arid climate in the study area.

5 RESULTS AND DISCUSSION

5.1 Quality assurance and control

The analyzed results obtained from the different laboratories were compared. One of the sample set showed great variation in the analysed results. The other sample set's results were similar with minimal variation. The variation witnessed in the former sample set analysis was attributed to storage and time between sample collection and analysis, which was possibly due long travel distance for analysis in South Africa.

5.2 Piezometric map

A comparison was made between water level and elevation. There was a great correlation between water levels recorded in the study area with elevation/topography. The graph in Figure 18 illustrates this correlation with an excellent correlation value of 0.9918. This correlation confirms works by authors (Key, 1983; Staudt, 2003) that the general water flow in the study area follows topography. The correlation may be unexpected in karst media. However, the digital elevation over the study area depicts the bowl-shaped morphology of Ramotswa aquifer with the high elevation ridges dipping towards the centre of the aquifer. Topography, which is influenced by geological structural controls, was also seen to be controlling water levels within the dolomitic sequence below the ground surface.

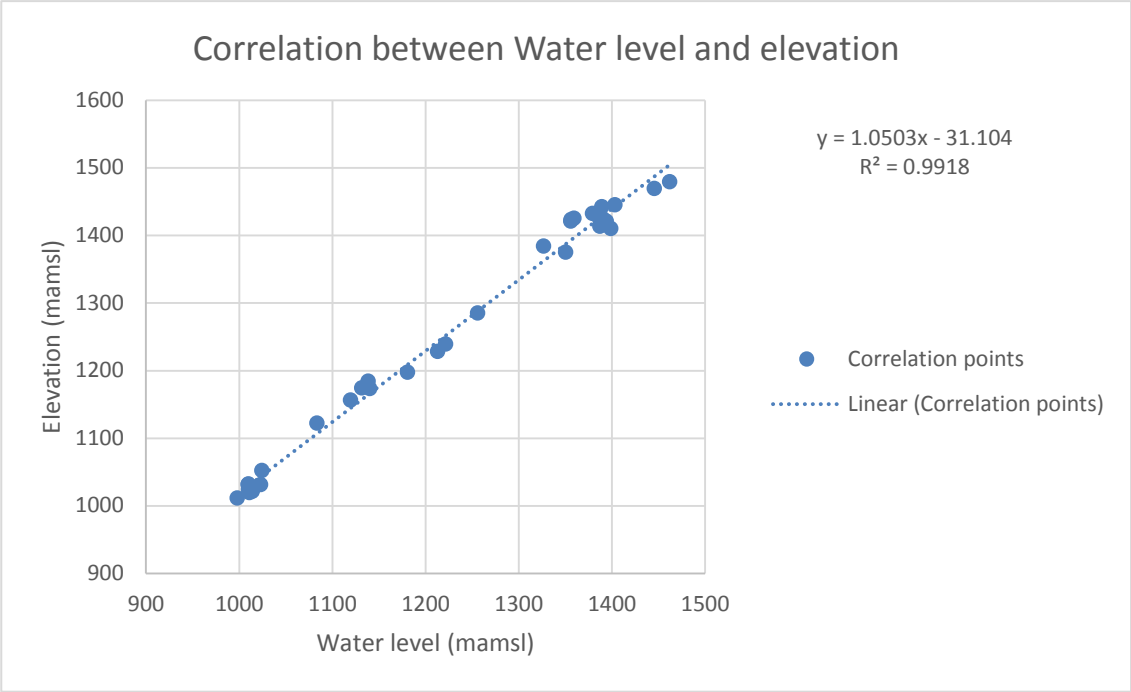

Figure 18. Correlation graph between water level and elevation.

The piezometric map (Figure 19) represents groundwater levels. This map suggests that flow within the aquifer is initially to the north, from the South African side in the south of the study area, and later moves in a north-easterly direction towards the village of Ramotswa in Botswana. This groundwater flow movement coincides with the topographic relief and drainage patterns, which goes from high elevation ridges in the south west to low topographic relief in the north easterly direction. The correlation graph of topography vs water levels has already alluded to this. In the majority of karst areas, groundwater is expected to be independent of topography. This is not the case here, as both geological structures and topography guide the regional orientation of the groundwater flow direction. Several authors (Burke *et al*., 1985and Clendenin *et al*., 1988) have mentioned the rift sequence with north-north-east trending grabens affecting the study area and the dolomitic sequence. It is the result of these structural elements that groundwater in this karst media flows and develops greatly in these pathways of less resistance. This matches the finding by Staudt (2003), who identified the general groundwater flow around the Ramotswa area to be in a north-northeastern direction. Subterranean connections following the network of faults must have also been established between the high lying areas and the low-lying areas to enable groundwater to flow in this north north-easterly direction. Knowing the direction of groundwater can assist in the general ecosystem management of the aquifer and in nitrate pollution management by indicating the pathway pollutants are most likely to travel.

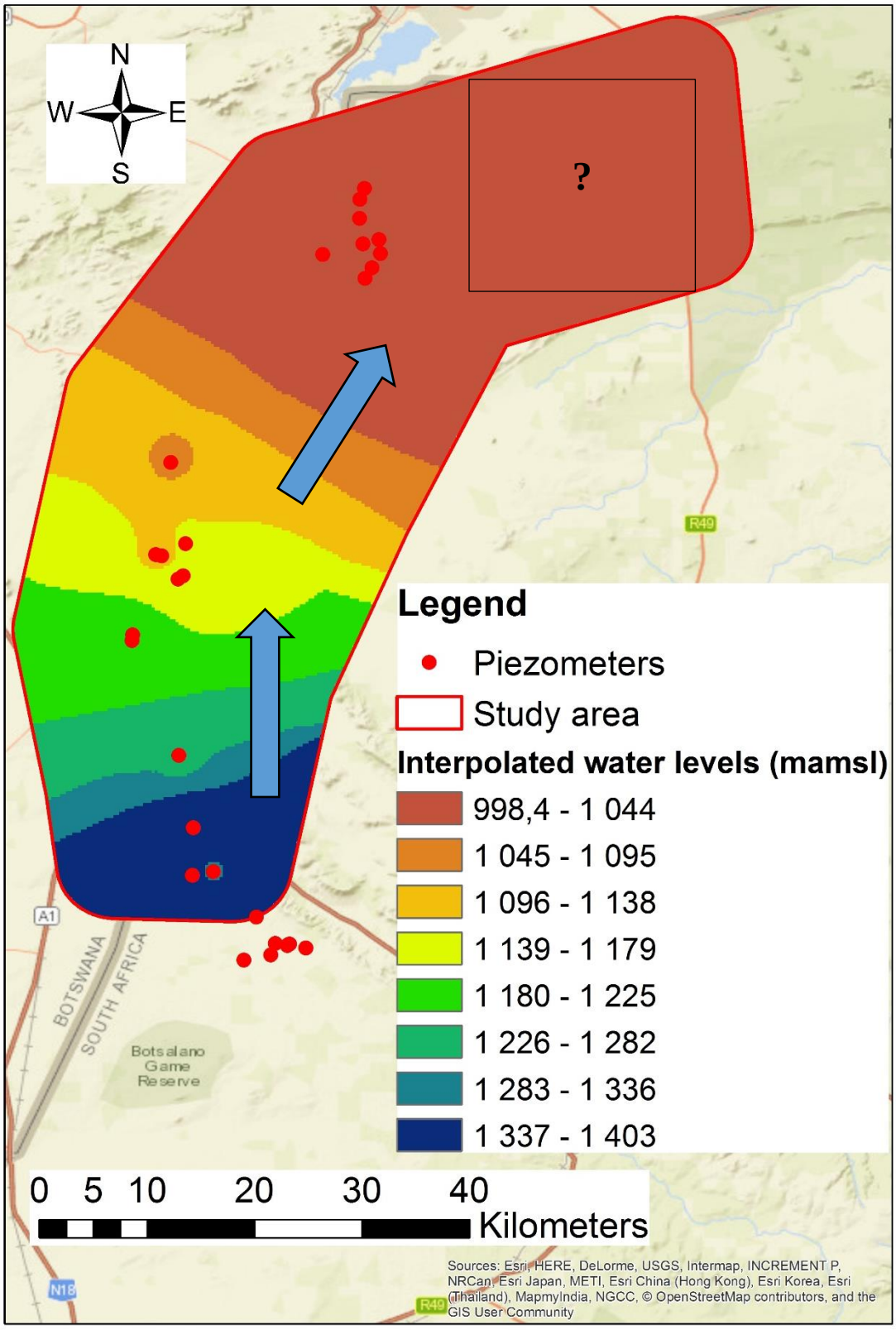

Figure 19. Piezometric map of the study area and indication the groundwater flow direction.

? = no recent water level data available.

Further to the east of the study groundwater flow direction cannot be interpolated due to lack of recent water level data in that region. However, the trend of total dissolved solids seems to suggest a possible direction. This will be elaborated in detail in the next section interpolating the groundwater flow direction using total dissolved solids.

The concentrations of Total Dissolved Solids (TDS) was used to further support the groundwater flow direction represented by the piezometric map. The illustration in Figure 20 shows low TDS values in the south-western region of the study area in South Africa. These TDS values increase gradually towards the north and eventually with the highest TDS values in the north-eastern region away from Ramotswa towards the village of Supingstad, South Africa, in the east. This increased TDS values could be indicative of prominent structural features such as faults, which were pronounced around the north eastern area, therefore increasing the degree of karstification and hence groundwater contact with country rock and movement. The trend of the groundwater flow direction suggested by the TDS trend flows the underground arcuate geometry of the Ramotswa dolomitic aquifer and moves in what appears to be a 'C' oriented movement, from South Africa in the south into Botswana in the north and back again into South Africa in the east.

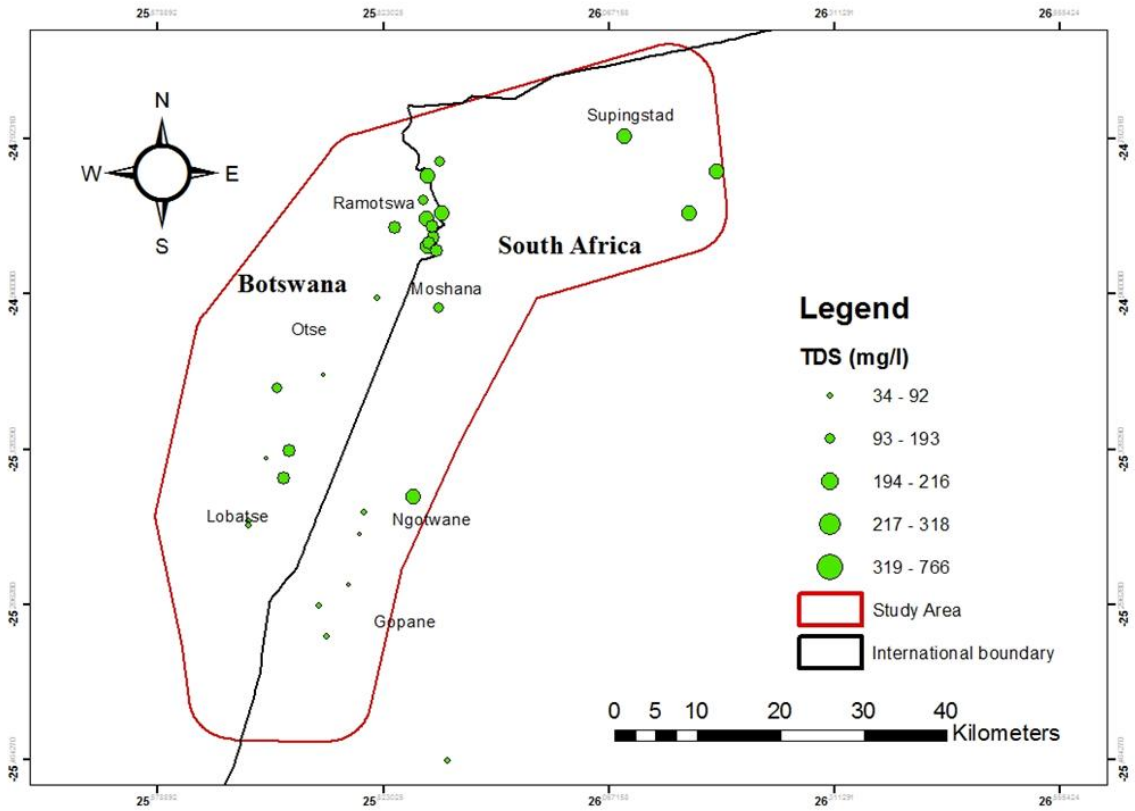

Figure 20. Spatial distribution of the total dissolved solids in the study area.

In some cases low TDS values could indicate 'high' rate of groundwater movement as a result of aquifer flushing, therefore this water has had less contact time with the country rock. Where the TDS values start increasing, this indicates an accumulation of dissolved minerals in the water carried from the point source of groundwater flow. This could also mean that where there is increased TDS, groundwater is moving at a slow rate and allowing the water more contact time with the country rock (dolomite). The TDS values follow a similar groundwater flow movement alluded by the piezometric map, which is a north north-easterly direction.

5.3 Groundwater pollution

The samples were analyzed for the sum of nitrate and nitrite in South Africa, whereas nitrate and nitrite was analyzed separately in Botswana. For simplicity of getting an understanding of the vulnerable sources of water supply, the sum of nitrate and nitrite was used across the entire study area.

Generally, nitrate and nitrite concentrations were below the WHO nitrate guideline limit of 50 mg/l as NO_3^-. There are two sample sites with concerning and alarming concentrations of the sum of nitrate and nitrite. The first concerning site was at sample ODI09ZA in Supingstad with a concentration of 45 mg/l, this is higher than the South African guideline limit of 20 mg/l. The Second alarming site was at BH287 in Ramotswa, located within the community, with a concentration of 99.9 mg/l nitrate. This was almost double the WHO and Botswana guideline limit for nitrate in drinking water.

An assessment of increased sum of nitrate and nitrite concentrations would have to take into account karst maturity, population density, rainfall amounts and a study of the surrounding environment. It is interesting to note that both sample sites with elevated sum of nitrate and nitrite concentrations are found in the north-easterly region of the study area, where groundwater levels are shallow in the region that receives the most amount of rainfall in the study. This means that natural retardation processes are not effective in removing nitrate from the polluted water and rainfall increases the concentrations. These sites are also located where the aquifer is more evolved (this will be discussed under geophysical survey analysis) therefore allowing pollutants to pass rapidly to the water table. The highly kasrtified and shallow water levels have also been identified by Ranganai *et al.* (2001) as contributing to groundwater pollution around Ramotswa village. An illustration of the spatial distribution of the sum of nitrate and nitrite across the study area is shown in Figure 21 below.

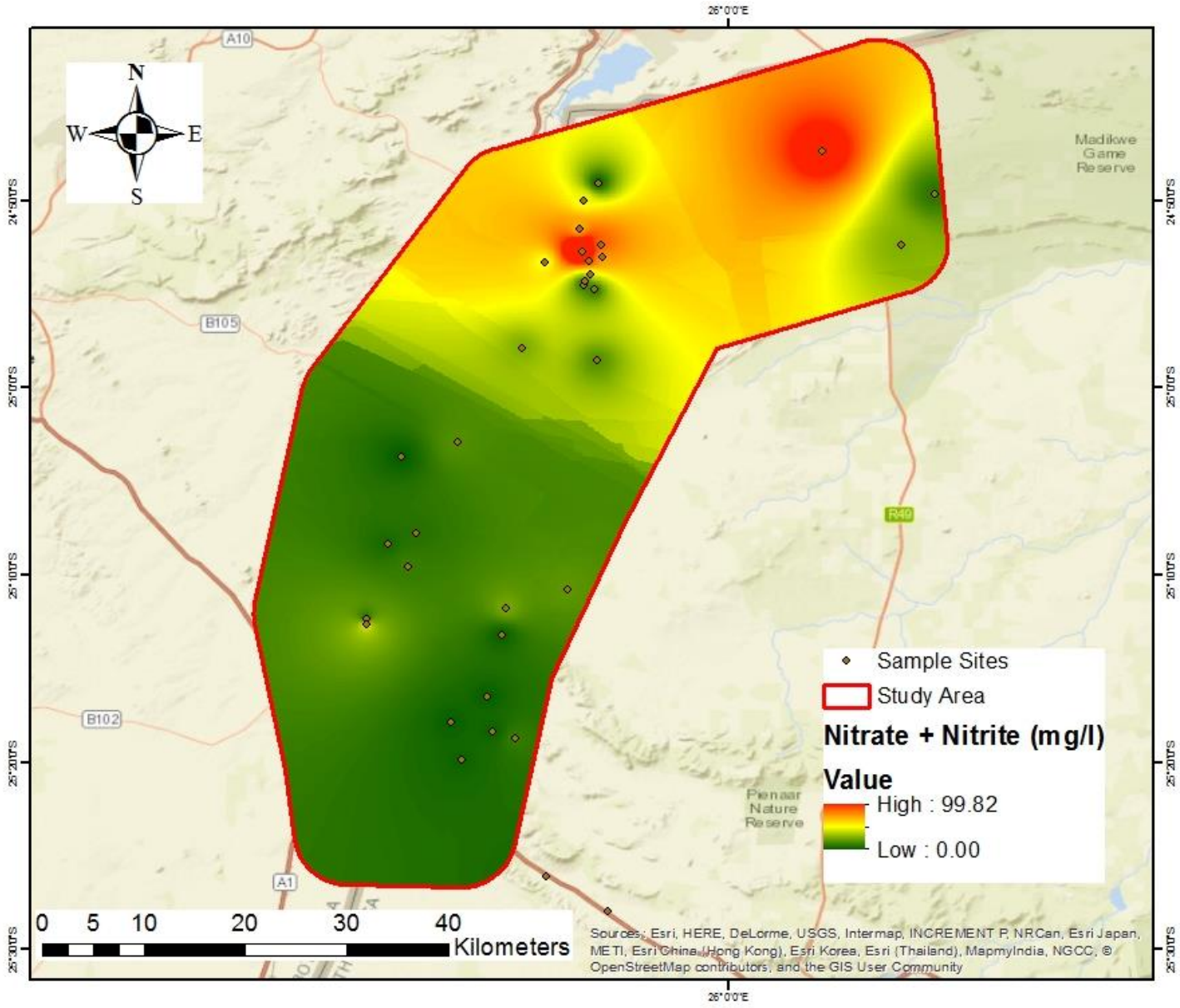

Figure 21. Spatial distribution of the sum of nitrate and nitrite

A comparison of historical nitrate concentrations data from the Department of Water Affairs Botswana and the concentrations recorded in this study was carried out. Four boreholes from this study matched those that have been analyzed previously by DWA Botswana and are compared in Figure 22. These were boreholes BH4975, BH9474, BH4348 and BH6424 for the years 2011 and 2012. For the years 2011 and 2012 the nitrate levels recorded follow a similar trend in all four boreholes. This may be because of the short period of time (9 month interval) which the analysis was carried out on the same borehole's groundwater. Not much land use change may have occurred in this short period of time, hence the similar results were obtained. However, there is a significant increase in nitrate

concentration in BH4348 from 45 to 69 mg/l between 2011 and 2012 which was over the WHO and Botswana guideline limits. The current study of the surrounding environment indicates that this could have been due to active agricultural activities that raised the nitrate concentration. The same borehole in 2016 records 15 mg/l. This decrease was because agricultural activities appear to have been long abandoned without any signs of active farming taking place and the nitrate maybe lost to groundwater by denitrification. BH4975 and BH6424 had increased nitrate concentrations recorded for the year 2016. For BH4975 field observations indicate no visible signs of pollution source. BH6424 is located in close proximity to a farmlands and the cemetery. This could either have been a more recent cemetery post 2012 or that the pollutants have only made their way to the groundwater in more recent years.

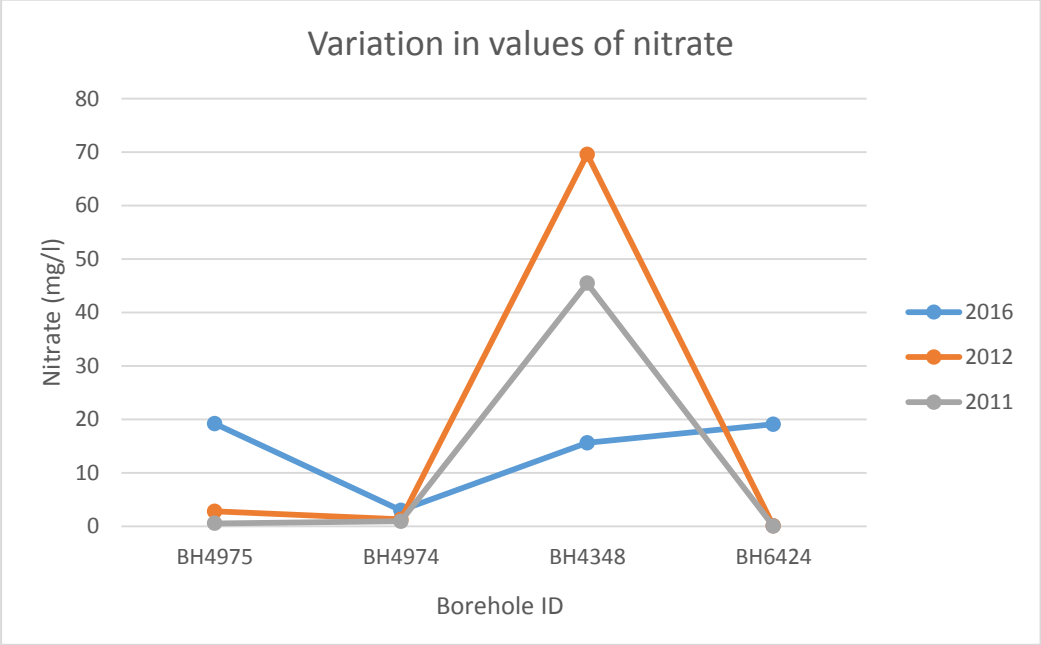

Figure 22. Comparison of the nitrate concentration values in boreholes in the years 2011, 2012 (DWA) and 2016.

5.4 Nitrate pollution sources

It is highly likely that anthropogenic sources are responsible for nitrate pollution in the study area because, the water quality at some boreholes exceeded the WHO and Botswana nitrate guideline limits. Bacterial indicators coupled with a study of the surrounding environment (see Appendix A) made it possible to decipher the source attribution of nitrate and nitrite pollution, besides the fact that it was anthropogenic. *E Coli.* and total coliforms aided in determining not only whether the pollution was recent or not, it also aided in identifying possible pathogens that may introduce risk to human health.

Samples sites with high *E. Coli* count by MPN/100ml were ODI03ZA with 83/100 ml counts and ODI04ZA with 401/100 ml counts. After consulting notes on the surrounding environment at these sites, it was concerning to know that sample site ODI03ZA is a community water supply tap. This high number of *E. Coli* count could be due to the nearby animal excreta from an abandoned kraal situated less than 100 m (see Figure 23) and from unlined pit latrines prominent in the local community. No visible potential pollutant source was identified for ODI04ZA as it is located in a natural environment. However, it appears that there was some form human settlement related to a small mining activity around the area in the past.



Figure 23. Sample site ODI03ZA showing the position of the community water tank near an abandoned animal kraal.

An illustration of the spatial distribution of *E. Coli* across the study area is depicted in Figure 24. Samples sites with high *E. Coli.* count by CFU/100 ml are significantly lower than those recorded by MPN/100 ml, this can be attributed to former method being an actual count while the latter is a statistical count. Sites BH4974 recorded 6/100 ml and BH287 4/100 ml *E. Coli* counts. Site study suggests that the presence of *E. Coli* found at these sites could be due

to a nearby abandoned dumpsite and old farm lands at BH4974. Unlined pit latrines within the community was a possible pollutant source for BH287.

Total coliform counts across sample sites (Figure 25) follow a similar trend to that of *E. Coli* with additional sample sites identified with presence of total coliform indicator where *E. Coli* counts were not picked up. Elevated numbers of total coliform were identified at the following samples: ODI03ZA 330/100 ml, ODI04ZA 2005/100 ml, BH287 200/100 ml, BH4974 51/100 ml and at sites ODI07ZA 201/100 ml, ODI08ZA 201/100 ml, ODI16 95/100 ml, where *E. Coli* was not picked up.

The sources of pollution at the additional sites identified by total coliform indicator coupled with the study of surrounding environment are as follows: ODI07ZA was used for domestic purposes and pit latrines were prevalent in this village with the potential pollution source less than 500 m from the private borehole; ODI08ZA was a private borehole located on the highly karstified region of the aquifer with the borehole situated in a goat kraal with abundant livestock excrement (Figure 26); ODI16ZA was a community tap located not far from the Notwane dam with potential pollutant sources being either pit latrines and or large scale agricultural activities taking place near the village.

Both bacteria sources of pollution identified across the study are typically non-point sources. These may prove difficult to manage considering the way the villages are already laid out and lack of regional water scheme pipelines that can mitigate the use of direct groundwater without water quality monitoring (particularly on the South African side of the study).

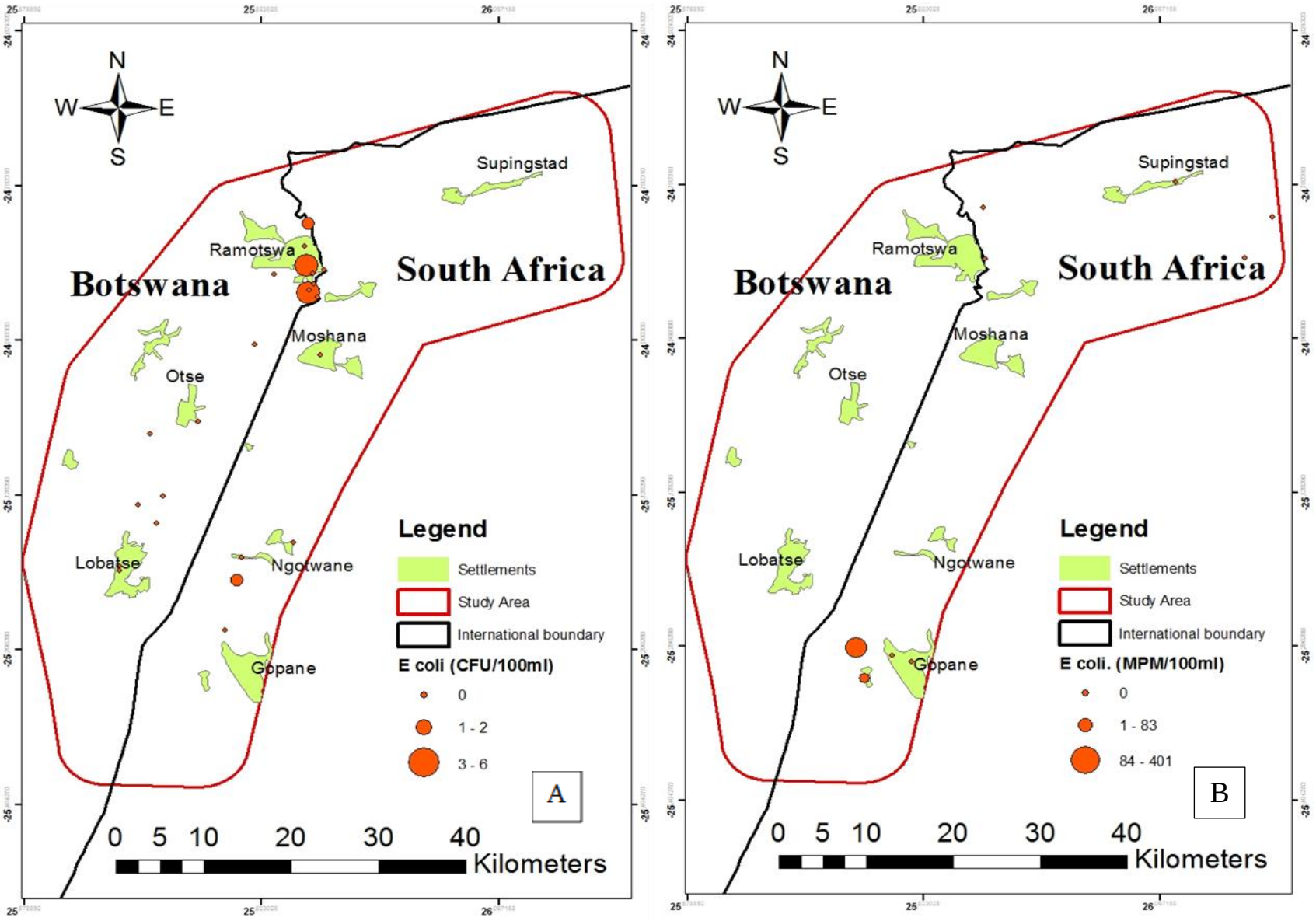

Figure 24. *E. Coli* counts at sample sites by (A) CFU/100 ml and (B) MPN/100 ml

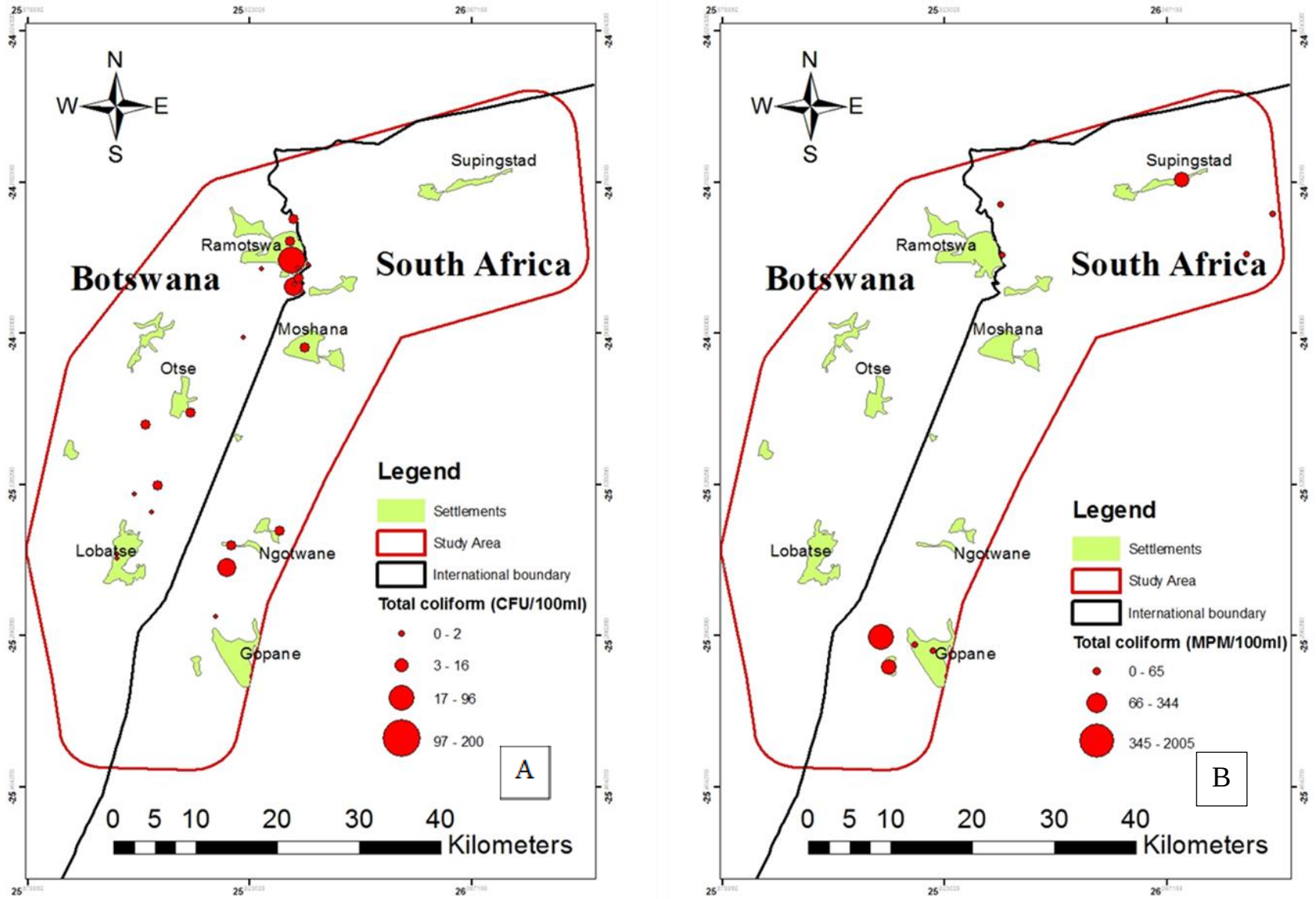

Figure 25. Total coliform count at sample sites by (A) CFU/100 ml and (B) MPN/100 ml.

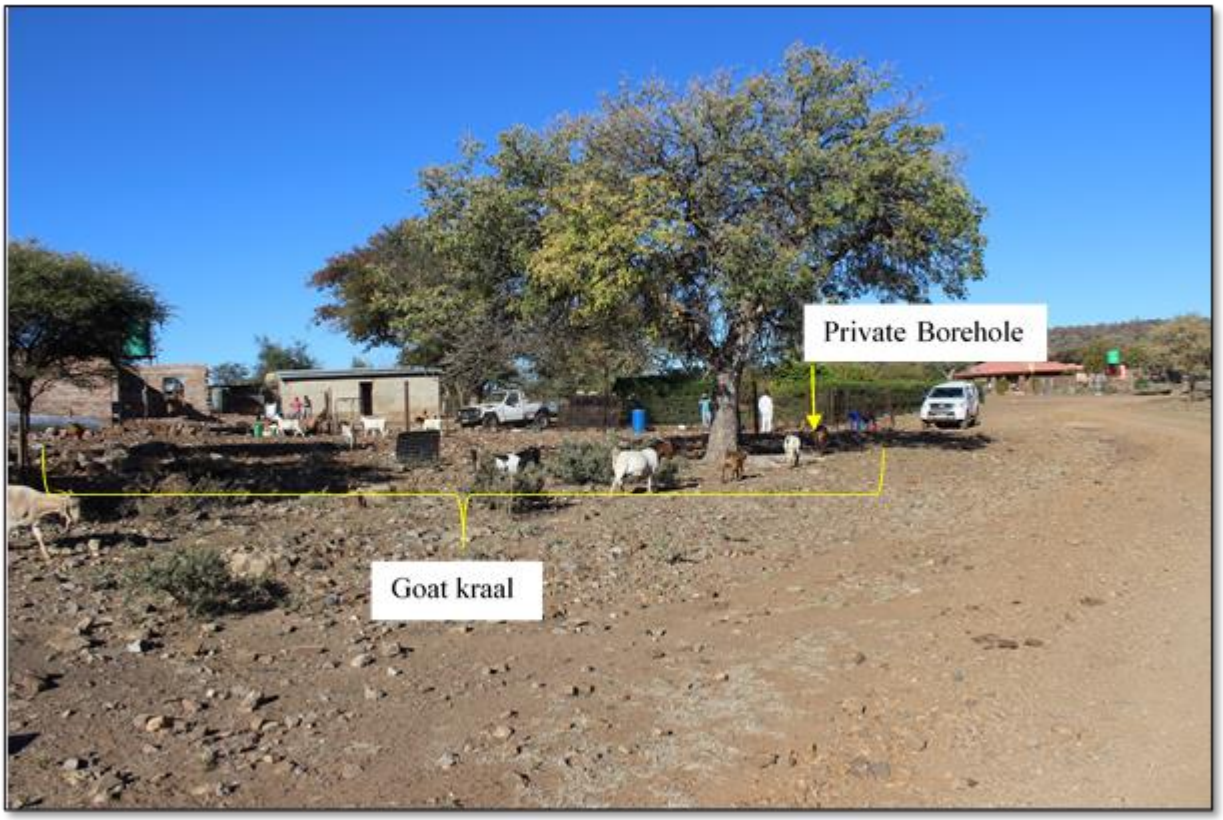

Figure 26. Goat kraal situated directly where private borehole is drilled in a highly karstified area (Supingstad, South Africa).

5.5 Groundwater pH

The pH levels (Figure 27) of the groundwater sampled in the study ranged from of 6.6 to 8.68. Majority of the values were above pH 7. This evidence proves that the controls on groundwater pH was that of the subsurface dolomite rock, therefore, influencing the alkalinity of the water. These alkaline values further confirm that the groundwater samples are indeed that of the Ramotswa dolomite aquifer because, the mineralogical composition of the aquifer's country rock has this effect on pH.

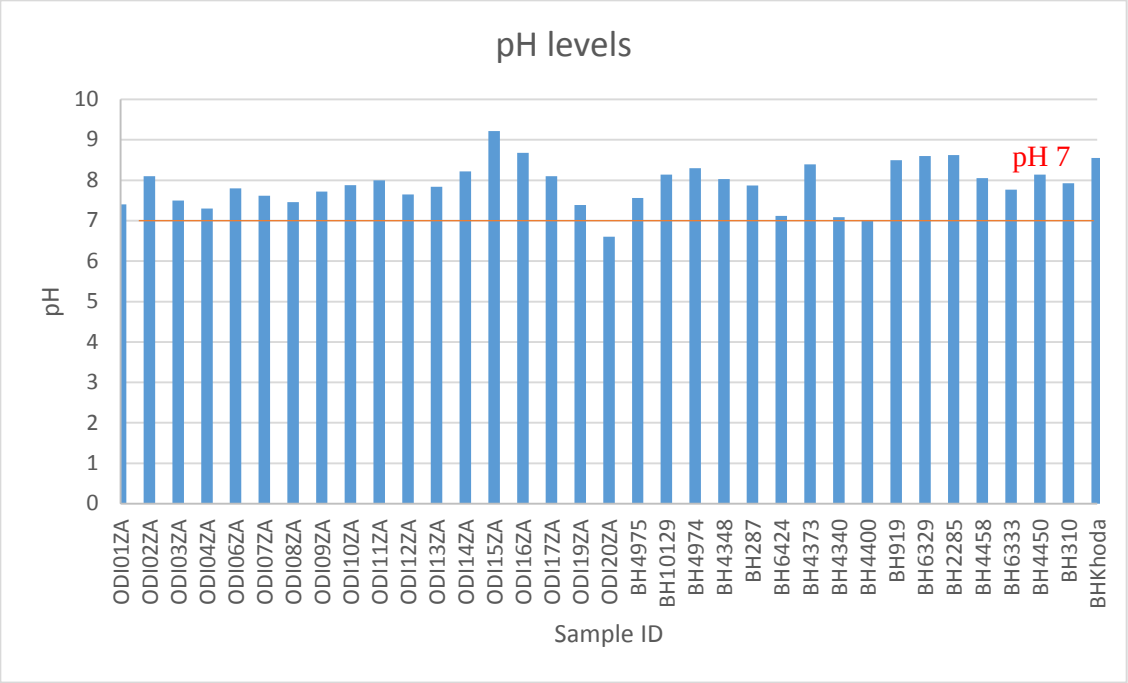

Figure 27. The water reaction (pH) levels at sample sites.

The observed groundwater temperatures range between 12 – 26.8 ˚C. These temperatures could possibly indicate fluctuation of the mean daily temperatures in the study area. Electrical conductivity values were extremely high with a record of 1227 µS/cm recorded at a sample site ODI08ZA, which is situated in Supingstad on the highly karstified area of the study. This indicates long groundwater residence time (long water- rock interaction time), wherein the rates of mineralization increase as a result. This high mineralization found in the groundwater had the people in the communities where the water was sampled complaining about the aesthetic taste of the water and damages caused to their water boiling appliances by this groundwater. A summary of the in-situ field parameters is tabled in Table 5 below.

Table 5. Summary of the in-situ field Parameters.

	Maximum	**Minimum**	**Mean**
Electrical Conductivity (µS/cm)	1227	17	414
Temperature (˚C)	27	12	22

5.6 Interpreted airborne geophysical survey results

The overall remnant magnetic field of fly area covering the study area is shown in Figure 28. This depicts the general magnetic field before interpretation of individual flight lines. The results of the interpreted airborne electromagnetic survey of the collapsed features are illustrated in Figure 29. These interpreted results appear as dashed lines due to the flight and tie lines flown over the study area (XRI Blue, 2016). It is difficult to join up these interpreted “dashed-lines” into collapse patterns due to a great degree of uncertainty in interpolating across areas that have not been surveyed.

The Ramotswa dolomitic aquifer basin baseline exhibits low remnant fields signatures, coloured in blue in Figure 28 below. Some linear east west and north east trending anomalies can be interpreted from the high remnant signatures as dyke features. These dyke features correspond with the structural geology identified in the region which control the direction and flow of groundwater.

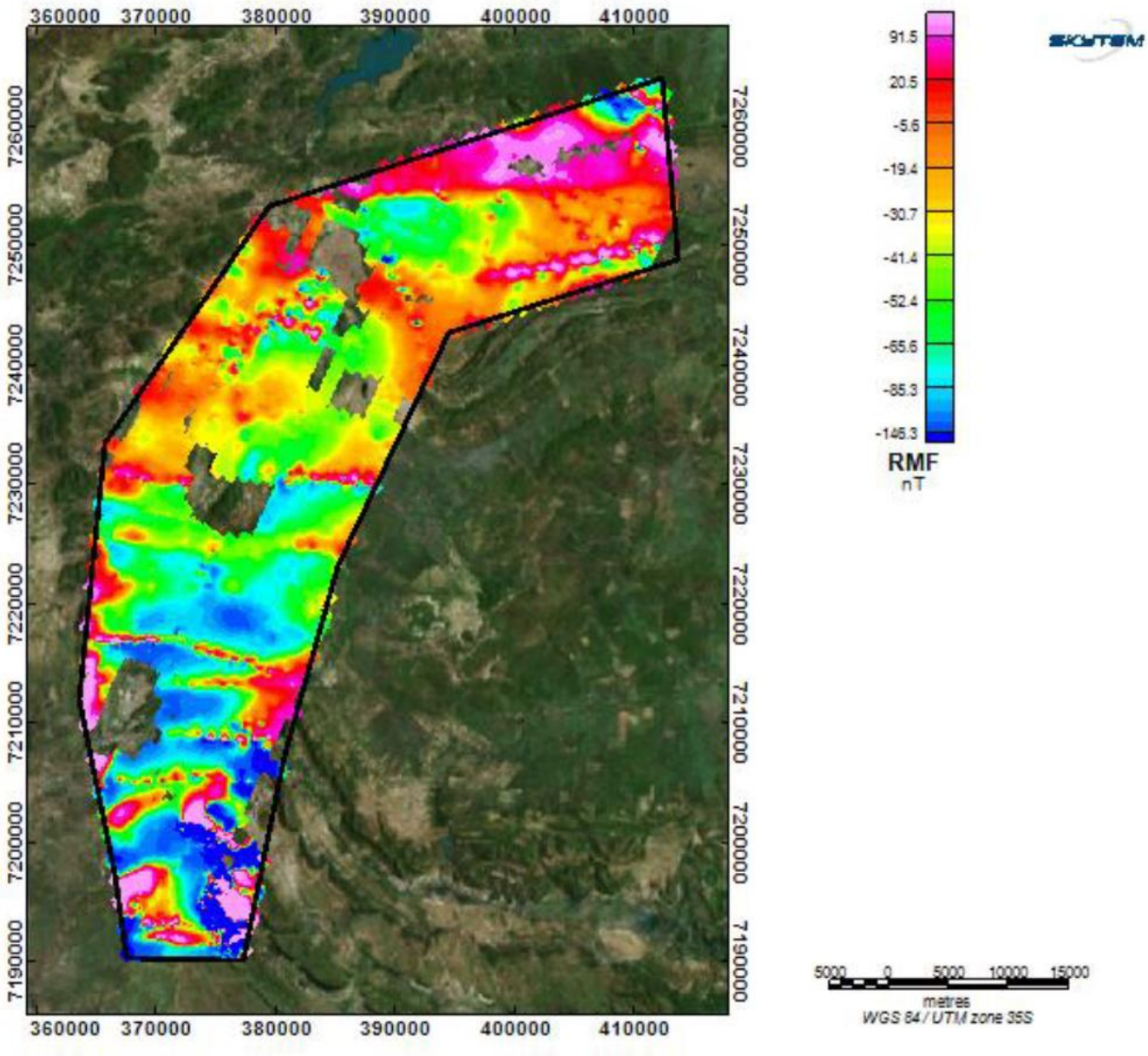

Figure 28. Remnant magnetic field of the fly zone in the study area (Source: XRI Blue, 2016).

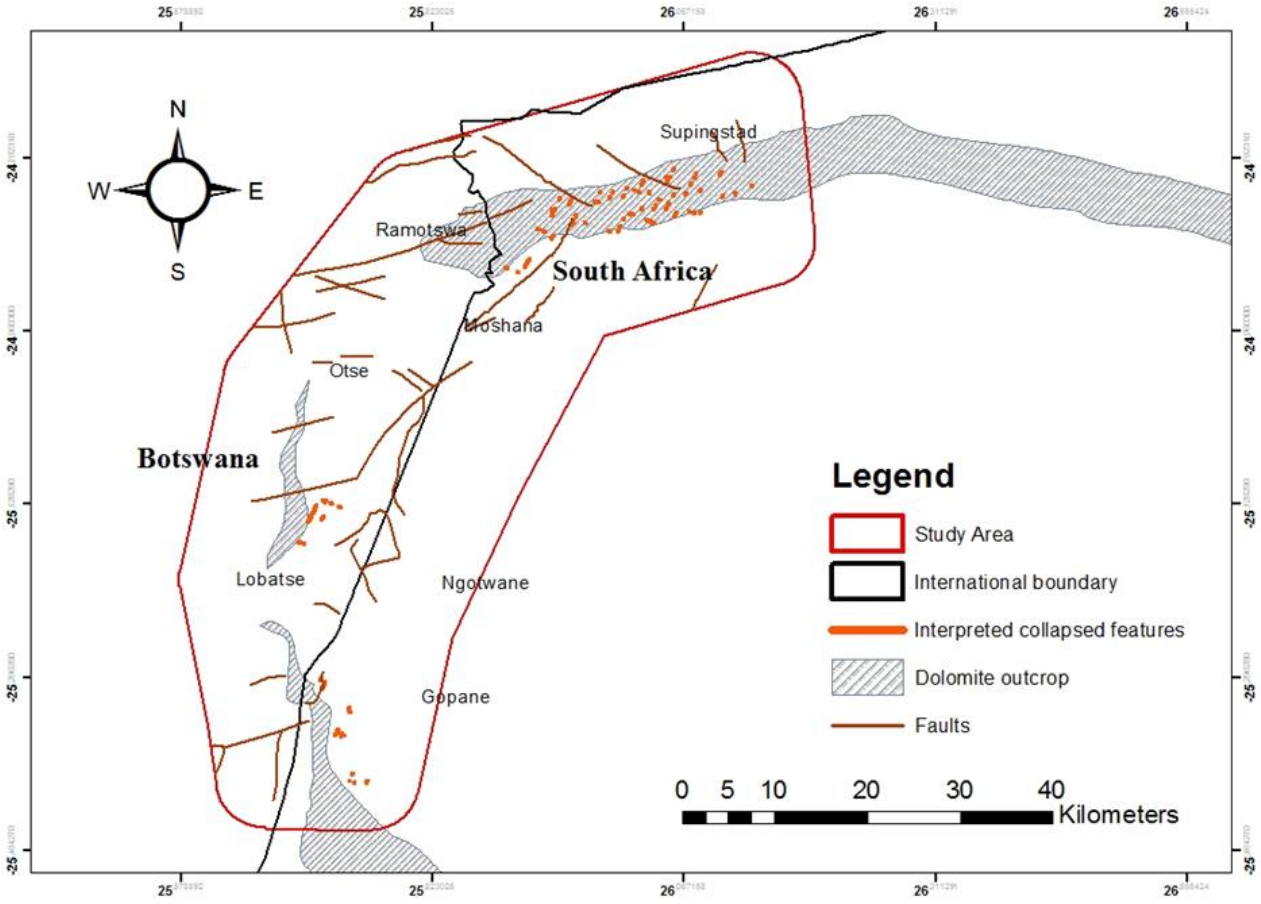

Figure 29. Interpreted collapsed features in the study (source: Council for Geoscience; Botswana Geoscience Institute; XRI Blue).

The collapsed features were more noticeable in the north-eastern region of the study area. These collapsed features correspond to the karst morphology of the Malmani Dolomites that Martini and Kavaliers (1976) termed the Bushveld type and thought to be of mature karst stage. There is great possibility that there are collapsed features in this region because of a number of factors contributing to karst development (Goldscheider *et al.*, 2007). Firstly, this eastern region of the study receives the greatest amount of rainfall and is of low elevation compared to the south-western region of the study. Secondly, faults cross cutting the dolomite outcrops on the surface create exposed secondary porosity channels for surface recharge (rainfall) to flow through and dissolution to take place. Both the presence of surface flow, pre-existing fractures and flow distance to the aquifer create the perfect condition in which a karst system is capable of maturing and or evolving. Hence the collapsed features identified underground in the north-eastern region of the study area using geophysical methods. Further evidence of high mineralization in the north-eastern region mentioned earlier in the study

supports the presence of collapsed underground features. This is because high mineralization occurs where groundwater has had long residence time and eventually creating wider conduits in the area of influence.

5.7 Recession index (K) estimate

Daily spring discharge data over a 26-year period from the Dinokana spring was used in the RECESS program to generate the recession index (K), quantified in days per log cycle. The program gave a recession index of 295.7 days per log cycle. This represents the median value of all the recession segments analyzed for both summer and winter months. It is the period required for groundwater discharge at the spring to recede by one log cycle (Rutledge, 1998). This recession index is a useful hydraulic parameter to evaluate groundwater potential, particularly in a climate variable region such as South African and Botswana. The recession index can be used as an indicator for low flow conditions (Kienzle, 2006). This analysis benefits resource managers for water planning or implementation of water conservation measures. It is evident that the Dinokana spring was not affected by the drought of 2015 because of the high K value. A study by Kienzle (2006), in a similar climatic setting to the study, categorized a K value greater than 30 to have no threat of low flow in the future. The spring water is therefore not vulnerable to low flow in the near future.

5.8 Master recession curve

To generate the master recession curve, a combination of 50 values of LogQ vs time for the analyzed recession segments generated by CURV were plotted in the R.C 4.0 tool. The master recession curve (Figure 30) is a combination of recession segments, of periods of at least 15 days, into one continuous straight line. The gentle regression slope reflects the overall storage characteristics of the karst compartment of the spring. Based on the current knowledge of the Dinokana spring, the gentle slope of master recession curve characterizes the general storage of the dolomite compartment of the aquifer. This slope alludes to massive groundwater storage with constant moderate outflow. The moderate outflow from the spring was confirmed by the surrounding community within the Dinokana spring who praised it for its longevity and regular flow.

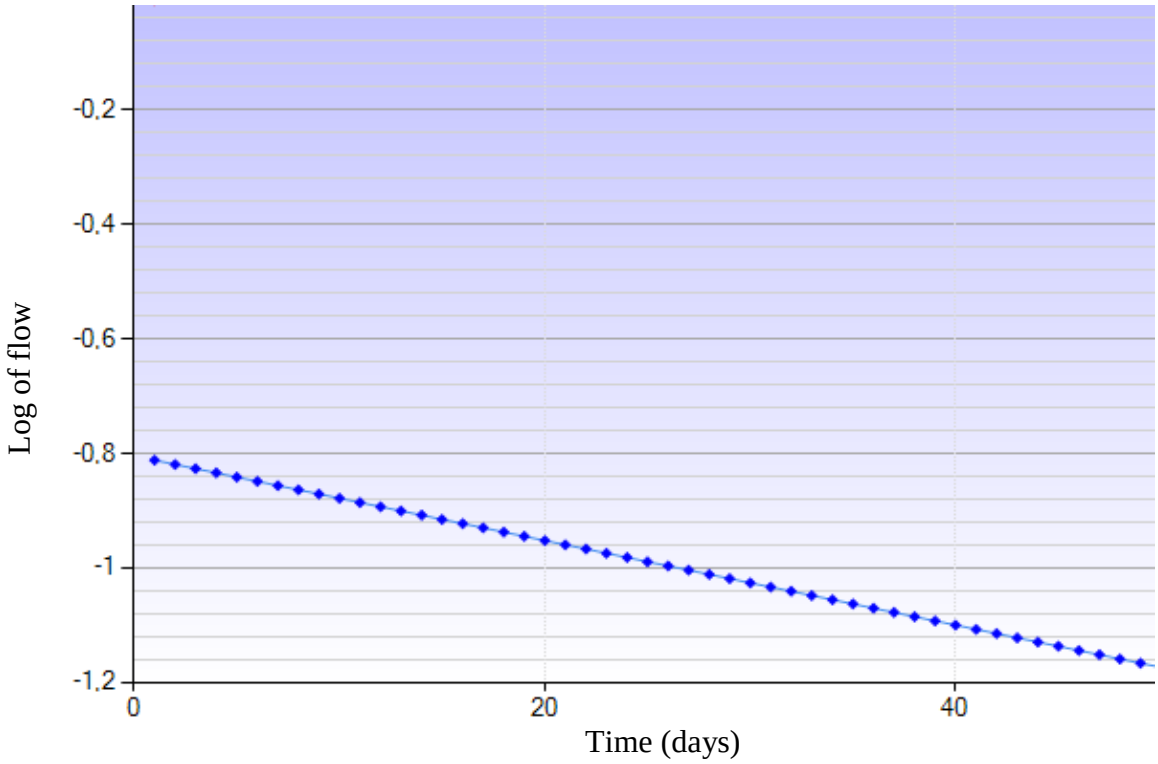

Figure 30. Master Recession Curve for the Dinokana spring from recession segments between 1990-2015; The regression slope reflects the storage characteristics.

6 CONCLUSION

The Ramotswa dolomitic transboundary aquifer is a very important source of water for both South Africa and Botswana. The aquifer forms part of the Notwane catchment in the Limpopo River Basin and comprises of the Malmani dolomitic sequence of the Chuniespoort Group. The aquifer is important for water storage and supply to the city of Gaborone in extremely dry conditions. Similarly, it is a vital source of water to rural communities, farmers and game reserves that rely directly on this groundwater resource in the absence of local water scheme pipelines in South Africa.

The Dinokana spring which forms part of the Malmani dolomite sequence has very active conduit networks that feed into the Notwane catchment. The spring's median recession index was calculated at 295.7 days per log cycle. This means that the spring is highly productive and not vulnerable to low flow in future. Very high storage properties are alluded to by the gentle slope of the generated MRC. This part of the Ramotswa aquifer where the Dinokana spring is compartmentalized has excellent potential and continuous to benefit both the ecosystem and community.

Groundwater flow direction correlates with the topographic relief in a north-north-easterly direction. This groundwater flow was also governed by both structures and geometry of the dolomite aquifer. The groundwater flow direction represented by piezometric map was supported by salinity trends alluding to the observed piezometric flow direction.

Nitrate pollution was prevalent due to the legacy of unlined pit latrines, particularly where there was shallow water table, high karstification, dense population and where high rainfall patterns were identified. Advection is the dominant form of pollutant migration. Sources of the nitrate pollution were deciphered with the aid of both microbiological indicators (*E. Coli* and total coliform) together with a study of the surrounding environment. Pollution was dominantly anthropogenic and typically from non-point sources with the use of pit latrines and livestock excrements contributing to the elevated nitrate concentrations. This means local communities, particularly those the north-eastern area of the study, need to take precautions when consuming groundwater from this more karstified region. The groundwater was more vulnerable to pollution.

Having established median recession index, groundwater flow and pollution, sufficient groundwater management practices can be designed and implemented to secure the groundwater resource. This will be to the benefit of both member states in a time of great climate variability more especially the communities of this region. This work contributes to the development of shared hydrogeological data which is significant to understanding transboundary aquifer resources as well as raise awareness on the vulnerability of the aquifer and the communities that are dependent on it.

7 RECOMMENDATIONS

The following recommendations are proposed to policy makers, governments and for further research to improve the understanding of the transboundary aquifer with regards to groundwater flow and pollution:

- A broader coverage, particularly in South Africa, and long term monitoring of water level and water quality should be carried out for a thorough understanding of flow patterns and pollution sources. A review of the water level monitoring sites needs to be considered in South Africa with the aim of monitoring the aquifer stress and flow patterns.
- Groundwater level monitoring should be conducted at points furthest away from communities and at observation wells furthest from production wells as well, even at a less frequent rate than boreholes closer to communities, for future trend analysis.
- A case by case groundwater quality risk assessment with a hazard approach should be designed and implemented. By laws should be reinforced regarding positioning of unlined pit latrines near communal water supply. Government should assist in the lining of pit latrines, prioritizing the highly karstified regions.
- Nitrogen isotope ($^{15}N/^{14}N$ and $^{18}O/^{16}O$) analysis, although expensive and not available locally, may be used to determine groundwater flow direction in the north eastern region to supplement the TDS results obtained.
- Recession index can be performed for summer and winter months to examine the effect of rainfall. The period of recession segments could be lengthened and analyzed for semi-arid climate together with the factors affecting recession. Genetic algorithm method can be employed in the construction of a master recession curve for a karst spring so that little information is lost due to averaging.

8 REFERENCES

Altchenko Y., Lefore N., Villholth K.G., Ebrahim G., Genco A., Pierce K., Woolf R., Mosetlhi B.B.T., Moyo T., Kenabatho P. & Nijsten G. (2016). Resilience in the Limpopo basin: The potential role of the Transboundary Ramotswa aquifer, Baseline report.

Anuraga, T. S., Ruiz, L., Mohan Kumar, M. S., Sekhar, M., & Leijnse, A. (2006). Estimating groundwater recharge using land use and soil data: a case study in South India. Agricultural Water Management, 84(1–2), 65–76.

Bechtel T.D., Bosch F.P., and Gurk M. (2007). In: Goldscheider, N. and Drew, D. eds. Methods in Karst Hydrogeology: IAH: International Contributions to Hydrogeology. Netherlands: Taylor & Francis, pp 171-199

Beger, K. (2001). Environmental Hydrogeology of Lobatse; South East District, Republic of Botswana, s.l.: Department of Geological Survey Botswana, Environmental Geology

Beukes, N.J., (1987). Facies relations, depositional environments and diagenesis in a major early Proterozoic stromatolitic carbonate platform to basinal sequence, Campbellrand Subgroup, Transvaal Supergroup, Southern Africa. Sedimentary Geology, 54(1), pp.1-46.

Botswana Bureau of Standards, (2009). BOS 32:2009, second edition. Drinking water standard-Specification. BOBS Gaborone.

Burke, K., Kidd, W. S. F., & Kusky, T. (1985). Is the Ventersdorp rift system of Southern Africa related to a continental collision between the Kaapvaal and Zimbabwe cratons at 2.64 Ga ago?. Tectonophysics, 115(1), 1-24.

Button, A. (1986). The Transvaal sub-basin of the Transvaal Sequence. In: Anhaeusser, C.R., Maske, S. (eds.) Mineral deposits of southern Africa. Geol. Soc. S. Afr., Johannesburg, pp. 811-817

Cimenti, M., Biswas, N., Bewtra, J. K., & Hubberstey, A. (2005). Evaluation of microbial indicators for the determination of bacterial groundwater contamination sources. *Water, air, and soil pollution*, *168*(1-4), 157-169.

Clendenin, C. W. (1989). Tectonic influence on the evolution of the early Proterozoic Transvaal Sea, Southern Africa. Ph.D. thesis. University of Witwatersrand, Johannesburg, South Africa.

Clendenin, C. W., Charlesworth, E. G., & Maske, S. (1988). An early Proterozoic three-stage rift system, Kaapvaal craton, South Africa. Tectonophysics, 145(1), 73-86.

Crockett, R. N. (1972). The Transvaal System in Botswana: its geotectonic and depositional environment and special problems. Trans. Geol. Soc. S. Afr, 75, 275-292.

d'Hydrogéologie, Centre d'Hydrogéologie, Université de Neuchâtel, 16:167–183.

Davies, J., Robins, N. S., Farr, J., Sorensen, J., Beetlestone, P., & Cobbing, J. E. (2013). Identifying transboundary aquifers in need of international resource management in the Southern African Development Community region. Hydrogeology Journal, 21(2), 321-330.

Department of Water Affairs (2004). Ramotswa Wellfield Allocation of Boreholes for Farming Purposes. Department of Water Affairs, Ground Water Division.

Dewey, J. F., & Burke, K. C. (1973). Tibetan, Variscan, and Precambrian basement reactivation: products of continental collision. The Journal of Geology, 683-692.

Dietvorst, E. J. (1988). Early Precambrian basement uplift and block faulting along the western margin of the Bushveld Complex, southeastern Botswana. Journal of African Earth Sciences (and the Middle East), 7(4), 641-651.

Dreybrodt, W. (1988). Limestone dissolution rates in karst environments. *Bulletin*

DWAF (DEPARTMENT OF WATER AFFAIRS AND FORESTRY, SOUTH AFRICA). (1996). South African Water Quality Guidelines (2nd ed.). Volume 1: Domestic Water Use.

Eriksson, K. A. and Truswell, J. F. (1974). Stratotypes from Malmani Subgroup northwest of Johannesburg, South Africa. *Transvaal Geological Society South Africa*. **77**. 211 – 222.

Eriksson, P. G., Altermann, W., & Hartzer, F. J. (2006). The Transvaal Supergroup and its precursors. The Geology of South Africa. Geological Society of South Africa, Johannesburg/Council for Geoscience, Pretoria, 237-260.

Eriksson, P. G., Hattingh, P. J., & Altermann, W. (1995). An overview of the geology of the Transvaal Sequence and Bushveld Complex, South Africa. Mineralium Deposita, 30(2), 98-111.

Eriksson, P. G., Schweitzer, J. K., Bosch, P. J. A., Schereiber, U. M., Van Deventer, J. L., & Hatton, C. J. (1993). The Transvaal sequence: an overview. Journal of African Earth Sciences (and the Middle East), 16(1), 25-51.

FAO, U. (2004). Drought Impact Mitigation and Prevention in the Limpopo River Basin: A Situation Analysis.

Ford, D. C., & Williams, P. W. (1989). Karst geomorphology and hydrology (Vol. 601). London: Unwin Hyman.

Foster, S.S.D. (1987). Fundamental concepts in aquifer vulnerability, pollution risk and protection strategy. –TNO Committee on Hydrological Research, Proceedings and Information. 38, 69-86, Den Haag.

Gieske, A. and Gould, J. (1994). *INTEGRATED WATER RESOURCES MANAGEMENT WORKSHOP 1 994* (pp. 17-18). Departments of Environmental Science and Geology, University of Botswana.

Goldscheider, N. and Andre, B. (2007). Goldscheider, N., & Drew, D. (Eds.). Methods in Karst Hydrogeology: IAH: International Contributions to Hydrogeology, 26. CRC Press.

Goldscheider, N., Drew, D., & Worthington, S. (2007). Goldscheider, N., & Drew, D. (Eds.). Methods in Karst Hydrogeology: IAH: International Contributions to Hydrogeology, 26. CRC Press.

Groundwater. [online] Available at: http://www.karst-hydrogeology.de/iahkarst.html [20 November 2016]

Holland M., Witthüser, K. T., & Jamison A.A. (2010). The Karst System of the Cradle of Humankind World Heritage Site. WRC Report No. KV 241/10. Water Research Commission. Pretoria

IGRAC (2012). Transboundary aquifers of the world, 1: 50 000 000, update 2012. IGRAC,

International Association of Hydrogeologists, IAH. (1999). Karst Commission. n.d: Karst

Kaçaroğlu, F. and Günay, G. (1997). Groundwater nitrate pollution in an alluvium aquifer, Eskişehir urban area and its vicinity, Turkey. Environmental Geology, 31(3-4), pp.178-184.

Key, R. M. (1983). The geology of the area around Gaborone and Lobatse, Kweneng, Kgatleng, Southern and South East districts (Vol. 5). Geological Survey Department, Ministry of Mineral Resources & Water Affairs.

Kienzle, S. W. (2006). The use of the recession index as an indicator for streamflow recovery after a multi-year drought. *Water resources management*, *20*(6), 991-1006.

Lewis, W., Farr, J. L., & Foster, S. (1978). A detailed evaluation of the pollution hazard to village water-supply boreholes in Eastern Botswana. publisher not identified.

Martini, J. E. J., Eriksson, P. G., & Snyman, C. P. (1995). The Early Proterozoic Mississippi Valley-type Pb-Zn-F deposits of the Campbellrand and Malmani Subgroups, South Africa. Mineralium Deposita, 30(2), 135-145.

Martini, J., & Kavalieris, I. (1976). The karst of Transvaal (South Africa). International Journal of Speleology, 8(3), 1.

Meyer, R. (2014). Hydrogeology of groundwater region 10: The karst belt. WRC Report No. TT 553/14. Water Research Commission. Pretoria.

Moore, J. M., Tsikos, H., & Polteau, S. (2001). Deconstructing the Transvaal Supergroup, south Africa: implications for Palaeoproterozoic palaeoclimate models. Journal of African Earth Sciences, 33(3), 437-444.

Mpaetona, K. (2016). Floods cripple Ramotswa. [online] Available at: http://www.mmegi.bw/index.php?aid=58619&dir=2016/march/16 [20 September 2016].

Pietersen, K., Beekman, H. E., & Holland, M. (2011). South African Groundwater Governance Case Study. WRC Report No. KV 273/11. Water Research Commission. Pretoria.

Ranganani, R.T., Gotlop-Bogatsu, Y., Maphanyane, J. and Tladi, B. (2001). Hydrochemical and Geophysical Evaluation of Groundwater Pollution in the Ramotswa Wellfield, SE Botswana. *BIE2001 Technical Papers*, pp.193-200.

Rutledge, A. T. (1998). Computer programs for describing the recession of ground-water discharge and for estimating mean ground-water recharge and discharge from streamflow records: Update. US Department of the Interior, US Geological Survey.

Rutledge, A. T. (2007). Program User Guide for RORA. *US Geological Survey: Reston, VA, USA.*

Scott, T. M., Rose, J. B., Jenkins, T. M., Farrah, S. R., & Lukasik, J. (2002). Microbial source tracking: current methodology and future directions. *Applied and environmental microbiology*, *68*(12), 5796-5803.

Stadler, S., Talma, A. S., Tredoux, G., & Wrabel, J. (2012). Identification of sources and infiltration regimes of nitrate in the semi-arid Kalahari: Regional differences and implications for groundwater management. Water SA, 38(2), 213-224.

Statistics Botswana (2011). South East District- Population and Housing Census

Statistics South Africa (2011). Census statistics by place: Ramotshere Moiloa Local Municipality

Staudt, M. (2003). Environmental hydrogeology of Ramotswa. Lobatse, Botswana: Botswana Department of Geological Survey.

Steyn, L. (2015). Drought's devastating ripple effect. [online] Available at: http://mg.co.za/article/2016-01-14-droughts-devastating-ripple-effect [19 February 2017].

Tallaksen, L. M. (1995). A review of baseflow recession analysis. *Journal of hydrology*, *165*(1-4), 349-370.

Villholth, K. G., Tøttrup, C., Stendel, M., & Maherry, A. (2013). Integrated mapping of groundwater drought risk in the Southern African Development Community (SADC) region. Hydrogeology Journal, 21(4), 863-885

Walraven, F., Armstrong, R. A., & Kruger, F. J. (1990). A chronostratigraphic framework for the north-central Kaapvaal craton, the Bushveld Complex and the Vredefort structure. Tectonophysics, 171(1), 23-48.

Wang, B., Strelakos, P. M., & Jokela, B. (2000). Nitrate source indicators in ground water of the Scimitar Subdivision, Peters Creek area, Anchorage, Alaska. US Department of the Interior, US Geological Survey.

Weaver, J. M., Cave, L., & Talma, A. S. (2007). Groundwater Sampling. Water Research Commission Report No. TT, 303(07).

WHO (WORLD HEALTH ORGANISATION) (1998) Guidelines for Drinking-Water Quality (2nd edn.). Appendum to Vol. 2. Health criteria and other supporting information, 64-80, WHO, Geneva.

XRI Blue (2016). Geophysical QA/QC corrected and final inverted AEM data Report for the development of subsurface mapping for the Trans-boundary Ramotswa aquifer that is part of the Limpopo river basin, using airborne geophysics. XRI Report.

Appendix A: Well site description

Well/sample site description																		
Sample site ID	Primary use of well:				Well condition:		Land use type:				Potential contamination source:				Domestic waste to:			
	Community	Domestic use	Production well	Observation well	Fenced	Well covered	Urban	Rural	Natural	Agriculture	Septic tank	Pit latrines	Fertilized fields	Non-visible /other	Septic tank	Sewer system	Pit latrines	Other
BH4400			X		X	X		X				X					X	
BH4340			X		X	X			X					X				X
BH4373			X		X	X			X					X				X
BH6424				X		X		X						X			X	
BH4337			X		X	X			X			X					X	
BH4995				X		X				X			X				X	
BH287				X		X		X				X				X		
BH4348				X		X			X				X				X	
BH4974				X		X		X					X					X
BH10129				X		X		X			X				X			
BH4975				X		X			X					X				X
BH6329				X		X			X					X				X

Well/sample site description																	
Sample site ID	Primary use of well:				Well condition:		Land use type:				Potential contamination source:				Domestic waste to:			
	Community	Domestic use	Production well	Observation well	Fenced	Well covered	Urban	Rural	Natural	Agriculture	Septic tank	Pit latrines	Fertilized fields	Non-visible /other	Septic tank	Sewer system	Pit latrines	Other
BH2285			X		X	X	X							X		X		
BH919				X		X	X							X		X		
BH4450				X		X			X					X				X
BH4458				X		X			X					X				X
BH6333				X		X			X					X				X
BH310	X				X	X			X					X				X
BHKHODA		X			X	X				X				X			X	
ODI01ZA		X			X	X		X				X					X	
ODI02ZA		X			X	X		X			X				X			
ODI03ZA	X				X	X		X				X			X			
ODI04ZA	X				X				X					X				X
ODI06ZA		X			X	X					X					X		

Well/sample site description																		
Sample site ID	Primary use of well:				Well condition:		Land use type:				Potential contamination source:				Domestic waste to:			
	Community	Domestic use	Production well	Observation well	Fenced	Well covered	Urban	Rural	Natural	Agriculture	Septic tank	Pit latrines	Fertilized fields	Non-visible /other	Septic tank	Sewer system	Pit latrines	Other
ODI07ZA		X			X	X		X				X					X	
ODI08ZA		X			X	X		X						X			X	
ODI09ZA		X			X	X		X				X					X	
ODI10ZA		X			X	X				X				X			X	
ODI11ZA		X			X	X		X						X	X			
ODI12ZA		X			X	X			X					X	X			
ODI13ZA		X			X	X			X					X			X	
ODI14ZA		X			X	X		X						X			X	
ODI15ZA	X					X			X					X				X
ODI16ZA	X				X	X		X				X					X	
ODI17ZA		X			X	X				X			X		X			
ODI19ZA	X					X			X					X			X	
ODI20ZA		X			X	X		X				X					X	

Appendix B: Water level sites and readings

Piezometer ID	Water Level (mbgl)	Elevation (mamsl)	Latitude	Longitude
DK24	1389,18	1442	-25,46718	25,82164
DK1	1394,19	1421	-25,47295	25,79251
D4N1662	1379,26	1432	-25,46719	25,82178
D4N1663	1356,13	1423	-25,46386	25,80811
D4N1659	1356,01	1421	-25,46511	25,80625
D4N1660	1359,46	1425	-25,46431	25,80736
D4N2519	1387,1	1413	-25,46336	25,79628
D4N2627	1387,15	1423	-25,44153	25,78028
D4N1665	1390,57	1424	-25,47742	25,76981
08-71477	1326,73	1384	-25,40356	25,74431
2526CC00014	1445,52	1469	-25,81578	26,04908
2525BCV0026	1350,3	1375	-25,40649	25,72660
2525DB00009	1398,8	1410	-25,62083333	25,975
2526CC00015	1 462	1479	-25,82139	26,045603
2525BCV0014	1256,1	1285	-25,30650	25,71557
2525BCV0017	1403,2	1 445	-25,36683	25,72739
BH4466	1119,48	1156	-25,13994	25,70127
BH4458	1180,85	1197	-25,15933	25,71485
BH6060	1138,49	1184	-25,15644	25,71907
BH6333	1140,17	1173	-25,12969	25,72124
BH919	1221,63	1239	-25,20586	25,67701
BH2136	1213,06	1228	-25,2107	25,67632
BH6329	1131,68	1174	-25,13888	25,6962
BH4975	1013,97	1021	-24,83311	25,87078
BH10129	1023,1	1031	-24,85832	25,86679
BH4974	998,02	1011	-24,90841	25,87133
BH4348	1010,11	1024	-24,89946	25,87702
BH4341	1010,98	1019	-24,87588	25,88283
BH287	1010,13	1032	-24,87947	25,86945
BH4995	1009,72	1031	-24,84224	25,86691
BH6424	1024,3	1052	-24,88836	25,83583
BH4349	1015,67	1027	-24,88746	25,88428
BH4450	1083,41	1122	-25,06211	25,70864

Appendix C: Nitrate + Nitrite, E Coli, Total Coliform values of sample sites

Sample ID	Nitrate (mg/l)	Nitrite (mg/l)	Nitrate + Nitrite	E. Coli	Total Coliform	E Coli or Total Coliform Units
ODI01ZA	-	-	0,281	0	10	MPN/100ml
ODI02ZA	-	-	4,074	0	0	MPN/100ml
ODI03ZA	-	-	0,518	83	330	MPN/100ml
ODI04ZA	-	-	0,137	401	2005	MPN/100ml
ODI06ZA	-	-	0,353	-	-	-
ODI07ZA	-	-	0,156	0	201	MPN/100ml
ODI08ZA	-	-	45,434	0	201	MPN/100ml
ODI09ZA	-	-	7,002	0	6	MPN/100ml
ODI10ZA	-	-	0,115	0	0	MPN/100ml
ODI11ZA	-	-	34,829	0	2	MPN/100ml
ODI12ZA	-	-	3,012	0	0	MPN/100ml
ODI13ZA	-	-	10,756	0	43	MPN/100ml
ODI14ZA	-	-	1,701	-	-	MPN/100ml
ODI15ZA	-	-	0,1	0	2	Cfu/100ml
ODI16ZA	-	-	0,1	2	95	Cfu/100ml
ODI17ZA	-	-	9,718	0	9	Cfu/100ml
ODI19ZA	-	-	7,634	0	10	Cfu/100ml
ODI20ZA	-	-	6,891	0	11	Cfu/100ml
BH4975	19,2	0	19,2	1	12	Cfu/100ml
BH10129	27,7	0	27,7	0	16	Cfu/100ml
BH4974	2,98	0	2,98	6	51	Cfu/100ml
BH4348	15,6	3,52	19,12	0	15	Cfu/100ml
BH287	99,9	0	99,9	4	200	Cfu/100ml
BH6424	19,1	0	19,1	0	0	Cfu/100ml
BH4373	1,81	0	1,81	0	0	Cfu/100ml
BH4340	1,82	0	1,82	0	0	Cfu/100ml
BH4400	37	0	37	0	0	Cfu/100ml
BH4337	27,8	0	27,8	0	0	Cfu/100ml
BH919	0,329	0	0,329	0	0	Cfu/100ml
BH6329	1,17	0	1,17	0	0	Cfu/100ml
BH2285	19,8	0	19,8	0	0	Cfu/100ml
BH4458	4,25	0	4,25	0	0	Cfu/100ml
BH6333	2,49	0	2,49	0	13	Cfu/100ml
BH4450	0	0	0	0	10	Cfu/100ml
BH310	10,6	0	10,6	0	1	Cfu/100ml
BHKhoda	6,64	0	6,64	0	7	Cfu/100ml

Appendix D: In situ field parameters

Borehole I.D	pH	Temp.(˚C)	EC (µS/cm)	TDS (mg/l)
ODI01ZA	7,4	20,7	156	-
ODI02ZA	8,1	20,5	344	-
ODI03ZA	7,02	17,3	293	188,5
ODI04ZA	6,83	26,5	17,36	110,3
ODI07ZA	7,62	16,8	481	310
ODI08ZA	7,46	23,3	1227	766
ODI09ZA	7,72	19	857	512
ODI10ZA	7,88	15	332	212
ODI11ZA	8	21,5	676	432
ODI12ZA	7,65	16,3	543	354
ODI13ZA	7,84	22,9	1119	706
ODI14ZA	8,22	13,6	276	177,6
ODI15ZA	9,22	22,8	90,9	33,6
ODI16ZA	8,68	18,3	136,2	88
ODI17ZA	8,1	12	258	164,5
ODI19ZA	7,39	18	500	319
ODI20ZA	6,6	22,8	327	208
BH4458	8,05	22,4	478	306
BH6333	7,77	24,4	438	280
BH919	8,6	23	153,6	97,8
BH2285	8,62	22,3	235	149
BH6329	8,6	23	145,5	91,5
BH4975	7,56	22,6	781	500
BH10129	8,14	26,8	318	203
BH4974	8,3	22,4	512	12,56
BH4348	8,03	26,5	494	318
BH287	7,87	26,5	603	385
BH6424	7,12	25,9	340	217
BH4373	8,39	24,7	388	243
BH4340	7,09	24,4	473	302
BH4400	7	23,4	398	253
BH4337	-	-	-	-
BH310	7,93	24,3	289	184
BHKhodaAgencies	8,55	23,1	75,5	48,4
BH4450	8,14	23,5	331	214

Appendix E: CURV output

T	LogQcms	LogQcmskm	Qcms	Qcmsm
-0.20842	-0.81200	-5.06855	0.15417	0.00001
-3.88632	-0.81939	-5.07594	0.15157	0.00001
-7.33180	-0.82678	-5.08332	0.14901	0.00001
-10.54485	-0.83416	-5.09071	0.14650	0.00001
-13.52548	-0.84155	-5.09810	0.14403	0.00001
-16.27368	-0.84894	-5.10549	0.14160	0.00001
-18.78945	-0.85633	-5.11288	0.13921	0.00001
-21.07280	-0.86371	-5.12026	0.13686	0.00001
-23.12372	-0.87110	-5.12765	0.13455	0.00001
-24.94222	-0.87849	-5.13504	0.13228	0.00001
-26.52829	-0.88588	-5.14243	0.13005	0.00001
-27.88194	-0.89327	-5.14981	0.12786	0.00001
-29.00315	-0.90065	-5.15720	0.12570	0.00001
-29.89195	-0.90804	-5.16459	0.12358	0.00001
-30.54832	-0.91543	-5.17198	0.12150	0.00001
-30.97226	-0.92282	-5.17937	0.11945	0.00001
-31.16377	-0.93020	-5.18675	0.11743	0.00001
-31.12286	-0.93759	-5.19414	0.11545	0.00001
-30.84953	-0.94498	-5.20153	0.11351	0.00001
-30.34377	-0.95237	-5.20892	0.11159	0.00001
-29.60558	-0.95976	-5.21630	0.10971	0.00001
-28.63496	-0.96714	-5.22369	0.10786	0.00001

-27.43192	-0.97453	-5.23108	0.10604	0.00001
-25.99646	-0.98192	-5.23847	0.10425	0.00001
-24.32857	-0.98931	-5.24586	0.10249	0.00001
-22.42825	-0.99669	-5.25324	0.10076	0.00001
-20.29553	-1.00408	-5.26063	0.09906	0.00001
-17.93036	-1.01147	-5.26802	0.09739	0.00001
-15.33277	-1.01886	-5.27541	0.09575	0.00001
-12.50275	-1.02624	-5.28279	0.09414	0.00001
-9.44031	-1.03363	-5.29018	0.09255	0.00001
-6.14544	-1.04102	-5.29757	0.09099	0.00001
-2.61814	-1.04841	-5.30496	0.08945	0.00000
1.14158	-1.05580	-5.31235	0.08794	0.00000
5.13373	-1.06318	-5.31973	0.08646	0.00000
9.35830	-1.07057	-5.32712	0.08500	0.00000
13.81530	-1.07796	-5.33451	0.08357	0.00000
18.50473	-1.08535	-5.34190	0.08216	0.00000
23.42658	-1.09273	-5.34928	0.08077	0.00000
28.58085	-1.10012	-5.35667	0.07941	0.00000
33.96756	-1.10751	-5.36406	0.07807	0.00000
39.58669	-1.11490	-5.37145	0.07675	0.00000
45.43824	-1.12229	-5.37883	0.07546	0.00000
51.52222	-1.12967	-5.38622	0.07419	0.00000
57.83863	-1.13706	-5.39361	0.07294	0.00000
64.38746	-1.14445	-5.40100	0.07171	0.00000
71.16872	-1.15184	-5.40839	0.07050	0.00000

78.18240	-1.15922	-5.41577	0.06931	0.00000
85.42851	-1.16661	-5.42316	0.06814	0.00000
92.90704	-1.17400	-5.43055	0.06699	0.00000